Nonlinear Model Predictive Control with an Infinite Horizon Approximation

San Dinh, Yao Tong, Zhenyu Wei, Owen Gerdes and L. T. Biegler[1]
Department of Chemical Engineering
Carnegie Mellon University
Pittsburgh, PA 15213

Abstract

Current nonlinear model predictive control (NMPC) strategies are formulated as finite predictive horizon nonlinear programs (NLPs), which maintain NMPC stability and recursive feasibility through the construction of terminal cost functions and/or terminal constraints. However, computing these terminal properties may pose formidable challenges with a fixed horizon, particularly in the context of nonlinear dynamic processes. Motivated by these issues, we introduce an alternate moving horizon approach where the final element in the horizon is constructed from an infinite-horizon time transformation.

The key feature of this approach lies in solving the proposed NMPC formulation as an extended boundary value problem, using orthogonal collocation on finite elements. Numerical stability is ensured through a dichotomy property for an infinite horizon optimal control problem, which pins down the unstable modes, extending beyond open-loop stable dynamic systems, and leads to both asymptotic and robust stability guarantees. The efficacy of the proposed NMPC formulation is demonstrated on three case studies, which validate the practical application and robustness of the developed approach on real-world problems.

[1]Corresponding author: lb01@andrew.cmu.edu

1. Introduction

Model Predictive Control (MPC) has been widely deployed in the process industries and elsewhere. By solving an optimization problem on-line (1), it serves as a generic MIMO controller with direct handling of input and output constraints and can be adapted to a broad class of dynamic models. MPC is most widely developed for linear time invariant (LTI) models, either in step response (DMC) and state-space form. In addition, data-driven models [1] along with MPC variants with Hybrid Models [2] have been developed.

A particular development of MPC is the ability to incorporate *nonlinear first principle models* which offer a direct link to off-line planning and optimization. When successfully embedded within an on-line optimization framework, nonlinear model predictive control (NMPC) is able to operate over wide dynamic ranges (e.g., startup and shutdown), and can serve as a vehicle for Dynamic Real-time Optimization. On the other hand, fast NLP solvers and efficient implementations are needed for time-critical, on-line optimization. This is essential to reduce computational delay from on-line optimization, which may degrade NMPC performance [3].

We consider the model predictive control (MPC) problem for a discrete dynamic system with pre-defined sampling times, given as follows:

$$\begin{aligned}
\min \quad & \sum_{l=0}^{N-1} \psi(z_l, v_l) + \Phi(z_N) && \text{(1a)}\\
s.t. \quad & z_{l+1} = F(z_l, v_l), \quad l = 0, \dots N-1 && \text{(1b)}\\
& z_N \in \mathcal{X}_f, z_0 = x_k && \text{(1c)}\\
& z_l \in \mathcal{X}, v_l \in \mathcal{U}, \quad l = 0, \dots N-1 && \text{(1d)}
\end{aligned}$$

The dynamic model (1b) can be derived from a continuous-time ODE model,

i.e.,

$$\frac{dz}{dt} = f(z, v_l, t) \implies z_{l+1} = z_l + \int_{t_l}^{t_{l+1}} f(z, v_l, t')dt' \tag{2}$$

over a sampling time $\Delta t = t_{l+1} - t_l$. The plant state and control variables at discrete time $k = 0, \ldots, \infty$ are defined in their domains $x_k \in \mathcal{X}, u_k \in \mathcal{U}$ with z_l, v_l as the predicted states and controls indexed over the horizon $l = 0, \ldots, N$ at time k. Here, we consider stage costs $\psi(z_l, v_l)$ of tracking type, typically written as $\|z_l - x_s\|_Q^2 + \|v_l - u_s\|_R^2$ with setpoints (x_s, u_s), as well as a terminal cost $(\Phi(z_N))$ and a terminal region $\mathcal{X}_f$ to ensure stable performance. Problem (1) is solved over a horizon of N sampling times to determine the control variable $u_k = v_0$, which is injected at time k into the plant. Once u_k is injected, time advances with $k = k + 1$ and (1) is solved again.

Both performance and stability properties on MPC depend strongly on the length of the horizon N. Although generally considered intractable, it is well known [4] that the infinite horizon MPC ($N \to \infty$) has strong stability properties for linear and large classes of nonlinear models. On the other hand, stable performance can be ensured only if the states can be controlled within N finite steps. As a result, problem dependent approaches commonly select a sufficiently large N to balance stable performance with on-line computation costs, but without stability guarantees.

A number of approaches have been proposed to address these challenges. Limon et al. [5] analyzed the stability of MPC without terminal constraints. Instead, they show that by sufficiently weighting the terminal cost, the domain of attraction of the MPC controller is enlarged to (practically) the same domain of attraction of the MPC with terminal constraint, thus leading to an asymptotically stable controller. Also, Alamir [6] proposed a contraction-based NMPC formulation to accommodate short prediction horizons, also, without terminal state constraints. Instead, the underlying optimization problem is solved using

a standard cost function together with a stability-dedicated penalty term and no additional constraints. An interesting follow-on to this approach is presented in [7], which uses a time-varying penalty, at a sufficiently high rate, to stabilize an MPC horizon without terminal constraints. This concept was also extended to Economic Model Predictive Control in [8], where terminal constraints are avoided through penalization of increments between two successive states. Stability properties were shown and the size of the terminal region can be reduced by decreasing the sampling period for the same design parameter settings. Pannocchia et al. [9, 10] also obtained stability results for finite horizon NMPC without the need for terminal regions. Instead, a suitably large terminal cost was chosen for the control "cost-to-go" beyond the finite horizon. These properties were subsequently extended to include turnpike features for dissipative systems [11].

More recently, a supervisory scheme is developed in [12] that expands the closed-loop region of attraction for constrained linear-quadratic MPC without terminal constraints. Using the contraction concept, the controller dynamically alters the setpoint for the MPC problem so that the current state remains inside the region of attraction for the equilibrium point. Closed-loop stability can then be achieved with smaller prediction horizons and weighting parameters than with unsupervised MPC implementations. Moreover, contraction concepts from [6] have been integrated with an input-to-state (practical) stability property in [13] to develop stabilizing robust contraction-based MPC with variable prediction horizons. This approach is also free of terminal constraints, has easily updated terminal cost functions, and selects the shortest prediction horizon for closed-loop stability.

Moreover, related finite horizon formulations deal with the inclusion of terminal regions $\mathcal{X}_f$ that relax the endpoint constraint. Embedded within the ter-

minal region, a well-defined controller (e.g., linear-quadratic regulator) drives the state to its setpoint with a well-defined terminal cost. Once the state reaches the terminal region at the end of a sufficiently long finite horizon ($z_N \in \mathcal{X}_f$), the resulting MPC formulation inherits the stability properties of infinite horizon MPC. Numerous approaches have been developed for the construction of terminal regions, of various levels of accuracy [14, 15, 16, 17, 18]. Moreover, as shown in [19] and [20], the presence of constructed terminal regions is also useful in the development of NMPC strategies with adaptive finite horizons. Nevertheless, in most of these studies, a sufficiently large finite horizon is needed to guarantee reachability of the terminal region, often at the expense of added computational cost.

In this study, we consider an alternative approach that approximates an infinite horizon NMPC formulation based on the following NMPC subproblem solved at time t_k with plant state x_k:

$$
\begin{aligned}
V(x_k) = \min \quad & (\sum_{l=0}^{N-1} \psi(z_l, v_l) + \Phi(z_N))\Delta t && \text{(3a)}\\
s.t. \quad & z_{l+1} = F(z_l, v_l), z_0 = x_k \quad l = 0, \dots N-1 && \text{(3b)}\\
& z_s = \bar{F}(z_N, \bar{v}) && \text{(3c)}\\
& z_N, z_l \in \mathcal{X}, \bar{v}, v_l \in \mathcal{U}, \quad l = 0, \dots N-1 && \text{(3d)}
\end{aligned}
$$

with the desired steady state z_s. In the terminal segment the domain is $t \in [\bar{t}, \infty)$, where $\bar{t} = t_k + N\Delta t$ and $(\bar{z}, \bar{v})$ are the states and controls with:

$$
\bar{F}(z_N, \bar{v}) = z_N + \int_{\bar{t}}^{\infty} f(\bar{z}(t), \bar{v}(t))dt. \tag{4}
$$

As indicated in Problem (3) and illustrated in Figure 1, the terminal cost $\Phi(z_N)$ in (3) is constructed as an approximation to the infinite sum $\sum_{l=N}^{\infty} \psi(\bar{z}_l, \bar{v}_l)\Delta t$. This approach is based on concepts developed in the following background stud-

ies and is derived in more detail in Section 2.

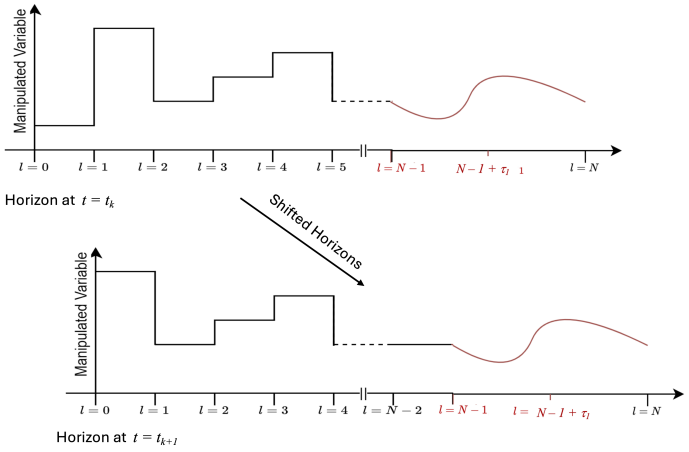

Figure 1: Manipulated variables in moving horizon with a terminal segment (in red) from $l = N - 1 \rightarrow N$. This terminal segment approximates an infinite horizon with a time transformation.

1.1. Background on Infinite Horizon Model Predictive Control

Keerthi and Gilbert [4] present the fundamental stability analysis for infinite horizon nonlinear MPC. A key assumption for this analysis requires nonlinear dynamics that have isolated state profiles along with unique linearizations that can be described with linear time varying (LTV) models. Both Controllability and Observability properties are assumed to prove asymptotic stability for infinite horizon problems with stage costs that are $\mathcal{K}_\infty$ functions of the states. Kunkel and Hagen [21] develop solution strategies for infinite time nonlinear optimal control problems. They introduce an exponential time transformation $\tau = exp(\gamma t)$ with decay constant $\gamma > 0$, and apply collocation at Gaussian points to solve the resulting boundary value problem and determine optimal trajectories. Marutani and Ohtsuka [22] propose a receding horizon algorithm with infinite horizon optimal control using a general time transformation, and

demonstrate its effectiveness on several nonlinear systems including the inverted pendulum problem. Würth and Marquardt [23, 24] apply a single shooting approach to infinite horizon NMPC problems that have open loop stable dynamics. They specifically apply a hyperbolic tangent time transformation, $\tau = tanh(\gamma t)$ with sampling times determined by wavelet adaptations. An extension of this work is presented in [25], which contrasts the infinite horizon approach with time transformation to a finite horizon turnpike approach.

Muehlebach and Andrea [26] consider an infinite horizon approach formulated with Galerkin approximations with either Laguerre (continuous) or Kautz (discrete) basis polynomials for dynamics on infinite horizons. An MPC formulation with LTI dynamics is developed with asymptotic stability and recursive feasibility properties. Their approach solves an inverted pendulum problem with much less effort than with finite horizon MPC. In a followup paper [27] they apply a fast active-set QP algorithm along with Bezier polynomials to deal with bounded profiles. This approach is demonstrated on UAV systems with 100 Hz performance. Also, Greer and Sultan [28] consider LTI MPC problems formulated with finite horizon (using a barrier QP for constraints) and infinite horizon parts, with no active constraints allowed in the latter. LQR control is used to derive terminal costs for the infinite horizon. The approach is demonstrated on fast helicopter control.

These previous studies develop infinite horizon MPC strategies that include concepts of time transformation, recursive feasibility, asymptotic stability, along with handling open loop instability. Our study combines all of these components to develop a novel infinite horizon NMPC approach. The next section reviews asymptotic stability properties for infinite horizon controllers, based on the discrete dynamic models considered in [4] and continuous time models in [29]. The infinite horizon NMPC formulation is derived and developed in Section 3, along

with an analysis of asymptotic and robust stability. Three NMPC case studies are presented in Section 4 along with a demonstration of the proposed approach, compared with finite horizon strategies. Section 5 summarizes the results of the paper and discusses areas for future work.

2. Stability of Infinite Horizon Controller

To deal with more general, open loop unstable systems in Problem (1), consider the dynamic optimization problem at time t_k without terminal conditions:

$$\min_{z_l, v_l} \quad \sum_{l=0}^{N-1} \psi(z_l, v_l) \tag{5a}$$

$$s.t. \quad z_{l+1} = F(z_l, v_l), \quad l = 0, \dots N-1, z_0 = x_k \tag{5b}$$

$$(z_l, v_l) \in \mathcal{X} \times \mathcal{U}, \quad l = 0, \dots N-1 \tag{5c}$$

Without loss of generality, we assume that $(z_s, v_s) = (0, 0)$. Moreover, we assume that the constraints represented by (5c) can be replaced by modifying the stage costs $\psi(z_l, v_l)$ with suitable penalty terms. In addition, for the dynamic system in (5), we invoke the assumptions from Keerthi and Gilbert [4], where (5b) is represented by 'linearized' LTV systems given by:

$$z_{l+1} = A_l z_l + B_l v_l, \quad (z_l, v_l) \in \mathcal{X} \times \mathcal{U} \subset \mathbb{R}^{n+m}, (0,0) \in int(\mathcal{X} \times \mathcal{U}) \tag{6}$$

with $A_l \in \mathbb{R}^{n \times n}, B_l \in \mathbb{R}^{n \times m}$, which are *uniformly completely controllable (UCC).* That is, for some $\mu_c, N > 0$, we have:

$$\sum_{j=0}^{N-1} \Psi(N, j+1) B_j B_j^T \Psi(N, j+1)^T \geq \mu_c I, \forall z_0 \in \mathcal{X}. \tag{7}$$

where $\Psi(i,j)$ is the state transition matrix given by $\Psi(i,i) = I$ and $\Psi(i,j) = A_{i-1} \times A_{i-1} \ldots \times A_j$ for discrete times $i > j$. Under UCC, the following theorem holds.

Theorem 1. *(Theorem 3.1 in [4]) Assume that, for all $l \geq 0$, the matrices A_l and B_l are uniformly bounded and that the pairs (A_l, B_l) are uniformly completely controllable for all $k \geq 0$. Then, there exists some $p_c > 0$ such that: for all $k \geq 0$ and $\|z_0\| \in \mathbb{R}^{n_x}$ there exists a sequence pair (x_k, u_k) which satisfies (5), (6) for $x_0 = z_0$, and $(x_{k'}, u_{k'}) = (0,0)$ for $k' \geq k + N$, and*

$$\sum_{l=0}^{N-1} \|(z_l, v_l)\| \leq p_c \|z_0\|. \tag{8}$$

Proof. From (6) we obtain:

$$\begin{aligned} z_{l+1} &= A_l z_l + B_l v_l = A_l(A_{l-1} z_{l-1} + B_{l-1} v_{l-1}) + B_l v_l \\ &= \Psi(l+1, l-1) z_{l-1} + \Psi(l+1, l-1) B_{l-1} v_{l-1} + B_l v_l \\ &= \Psi(l+1, 0)\ z_0 + \sum_{j=0}^{l} \Psi(l+1, j) B_j v_j \end{aligned} \tag{9}$$

with $z_N = \Psi(N,0)\ z_0 + D\hat{v}$ where $\hat{v} = [v_0^T, v_1^T, \ldots, v_{N-1}^T]^T$, $\Psi(l+1, j) = A_l A_{l-1} \ldots A_j$ and

$$D = [\Psi(N,0)B_0, \Psi(N,1)B_1, \ldots, \Psi(N, N-1)B_{N-1}].$$

By choosing $\hat{v} = D^T q$ and writing $0 = z_N = \Psi(N,0)\ z_0 + D\hat{v}$, we have from (9

$$-\Psi(N,0) z_0 \quad = \quad D\hat{v} = DD^T q \implies q = -(DD^T)^{-1} \Psi(N,0)\ z_0 \tag{10}$$

where DD^T is nonsingular from (7). As a result,

$$\|v_l\| \le \|\hat{v}\| = \|D^T q\| \le \|D\|\|(DD^T)^{-1}\|\|\Psi(N,0)\|\|z_0\|, \quad l = 0, \dots N-1 \quad (11)$$

and

$$\begin{aligned} \|z_l\| &= \|\Psi(l,0)z_0 + \sum_{j=0}^{l-1} \Psi(l,j)B_j v_j\| \le \|\Psi(l,0)\|\|z_0\| + \sum_{j=0}^{l-1} \|\Psi(l,j)B_j\|\|v_j\| \\ &\le (\|\Psi(l,0)\| + \sum_{j=0}^{l-1} \|\Psi(l,j)B_j\|\|D\|\|(DD^T)^{-1}\|\|\Psi(N,0)\|)\ \|z_0\| \qquad (12) \end{aligned}$$

are uniformly bounded. Moreover, from (11) and (12), we have:

$$\begin{aligned} \|(z_l, v_l)\| &\le \|z_l\| + \|v_l\| \le \|\Psi(l,0)\|\|z_0\| + [1 + \sum_{j=0}^{l-1} \|\Psi(l,j)B_j\|]\|v_j\| \\ &\le \left(\|\Psi(l,0)\| + [1 + \sum_{j=0}^{l-1} \|\Psi(l,j)B_j\|]\ \|D\|\|(DD^T)^{-1}\|\|\Psi(N,0)\| \right) \|z_0\| \end{aligned}$$

Summing this inequality over l leads to (8) with

$$p_c \ge \sum_{l=0}^{N-1} \left(\|\Psi(l,0)\| + [1 + \sum_{j=0}^{l-1} \|\Psi(l,j)B_j\|]\ \|D\|\|(DD^T)^{-1}\|\|\Psi(N,0)\| \right).$$

□

For state feedback stage costs $\psi(z_l, v_l)$, Theorem 1 leads to the following asymptotic stability property for infinite horizon control.

Theorem 2. *(paraphrase of Theorems 4.2 and 4.3 in [4]) In Problem (5), suppose that (5b) can be represented by (6) that satisfies UCC. Then for all $z(\bar{t}) \in \mathcal{X}$, there exist state feedback laws such that $\lim_{N\to\infty} z_N = 0$, which is the only equilibrium state of $z_{l+1} = F(z_l, v_l)$ and (5) is* uniformly asymptotically stable in the large. *Moreover, if the stage cost $\psi(z, v)$ is bounded below by a $\mathcal{K}$*

function $\alpha(\|z\|)$ *with state feedback control, then (5) is* exponentially stable.

Thus, for Problem (5) with $N \to \infty$, we assume UCC for state feedback stage costs, in order to guarantee well-posedness of Problem (1).

2.1. Existence and Well-posedness of Infinite Optimal Control in Continuous Time

Problem (3) includes a discrete time dynamic model as well as a terminal cost that incorporates dynamic behavior over infinite time. In order to develop the properties of (3), we also need to consider analogous stability properties in continuous time, for the terminal segment in (3). These require the analysis of nonlinear boundary value problems (BVPs) derived from optimality conditions of the terminal segment.

In general, existence and uniqueness properties of nonlinear BVP solutions can only be considered in a local sense [30], where the nonlinear system (5b) is represented as the LTV system (6) linearized about an isolated BVP solution $(\tilde{z}(t), \tilde{v}(t))$ that is assumed to exist. Existence and stability can then be shown for neighboring solutions to $(\tilde{z}(t), \tilde{v}(t))$. To this end, we consider the following control problem in continuous time, where the system dynamics (2) are linearized about $(\tilde{z}(t), \tilde{v}(t))$ and we redefine $z \leftarrow z - \tilde{z}$ and $v \leftarrow v - \tilde{v}$ for simplicity of notation. This leads to the optimal control problem for the terminal segment in Problem (3)

$$\min \quad \frac{1}{2}\int_{t_0}^{t_f} \left[z^T(t)\, Q(t)\, z(t) + v^T(t)\, R(t)\, v(t)\right] dt \tag{13a}$$

$$s.t. \quad \dot{z}(t) = A(t)\, z(t) + B(t)\, v(t) \tag{13b}$$

$$z(t_0) = z_N \tag{13c}$$

$$z(t_f) = 0 \tag{13d}$$

where we relabel $\bar{t}$ in (4) as t_0 and denote $t_f \to \infty$ as the terminal time. Through

suitable variable transformations, we assume that the terminal cost $\Phi(z_N)$ in (3 can be rewritten as (13a) with $Q(t)$ and $R(t)$ as symmetric positive semidefinite and definite matrices, respectively, for all $t \in [t_0, t_f]$. Also, $A(t) = \nabla_z f(\tilde{z}, \tilde{v})$, $B(t) = \nabla_v f(\tilde{z}, \tilde{v})$, and $f(z, v)$ is a continuously differentiable function. These LTV differential equations are related to the discrete difference equations (6) given above.

The optimality conditions of Problem (13) form a boundary value problem (BVP) that satisfies the *exponential dichotomy property* and "pins down the unstable modes." As stated below in Definition 5 and analyzed in Theorem 6, this property is essential to ensure well-posedness of the resulting BVP; this does not require stable open-loop dynamics. To derive the BVP corresponding to (13) we apply Pontryagin's maximum principle and define the Hamiltonian function as follows:

$$\begin{aligned} H(z(t), v(t), \lambda(t)) = \frac{1}{2}\left[z^T(t) Q(t) z(t) + v^T(t) R(t) v(t)\right] \\ + \lambda^T(t)\left[A(t) z(t) + B(t) v(t)\right] \end{aligned} \tag{14}$$

where the $\lambda(t)$ are costate variables. The first-order necessary conditions for optimality lead to the optimal feedback control:

$$\frac{\partial H(z(t), v(t), \lambda(t))}{\partial v} = 0 \Rightarrow v^*(t) = -R^{-1}(t) B^T(t) \lambda(t) \tag{15}$$

and a Hamiltonian BVP with the dynamics in the matrix form of:

$$\begin{bmatrix} \dot{z}(t) \\ \dot{\lambda}(t) \end{bmatrix} = \begin{bmatrix} \frac{\partial H(z(t), v(t), \lambda(t))}{\partial \lambda} \\ -\frac{\partial H(z(t), v(t), \lambda(t))}{\partial \mathrm{z}} \end{bmatrix} = \begin{bmatrix} A(t) & -S(t) \\ -Q(t) & -A^T(t) \end{bmatrix} \begin{bmatrix} z(t) \\ \lambda(t) \end{bmatrix} \tag{16}$$

where $S(t) = B(t) R^{-1}(t) B^T(t)$. From [29, 31] we exploit the linear relation between the optimal state and costate variables as $\lambda(t) = K(t) z(t)$, and obtain

the Riccati differential equation as follows:

$$\dot{K}(t) = -A^T(t)K(t) - K(t)A(t) + K(t)S(t)K(t) - Q(t). \tag{17}$$

The following definitions and theorems develop the stability properties of the Hamiltonian BVP with separated boundary conditions.

Definition 3. *(Controllability) The system (13b) is uniformly completely controllable if and only if the symmetric matrix*

$$\Omega(t, t_1) = \int_t^{t_1} \bar{\Psi}(t, \tau) B(\tau) B^T(\tau) \bar{\Psi}^T(t, \tau) d\tau \tag{18}$$

is positive definite for some $t_1 > t, \forall \mathrm{t} \geq t_0$, where $\bar{\Psi}(\cdot, \cdot)$ denotes the (continuous time) state transition matrix of the system (13b).

Note that this well-known condition is the continuous-time analog of UCC (7)and leads to a boundedness property (Proposition 5.2 in [32]) analogous to Theorem 1.

Theorem 4. *Under the assumption of uniform complete controllability, the solution set of (17) contains*

- *a unique symmetric positive definite root $P(t)$ such that the system $\dot{\sigma}(t) = [A(\mathrm{t}) - S(t)P(t)]\sigma(t)$ is uniformly asymptotically stable in forward time, and*
- *a unique symmetric negative definite root $N(t)$ such that the system $\dot{\rho}(t) = [A(t) - S(t)N(t)]\rho(t)$ is uniformly asymptotically stable in reverse time.*

Proof. See Appendix A for proof.

Definition 5. *(Exponential dichotomy) [29] The Hamiltonian BVP is said to have exponential dichotomy if there exist positive constants α_f, α_r, β_f and β_r*

such that for all $t \geq t_0$*:*

$$|z(t)| + |\lambda(t)| \leq \alpha_f e^{-\beta_f (t-t_0)}, \begin{bmatrix} z(t_0) \\ \lambda(t_0) \end{bmatrix} \in Y \tag{19a}$$

$$|z(t)| + |\lambda(t)| \geq \alpha_r e^{\beta_r (t-t_0)}, \begin{bmatrix} z(t_0) \\ \lambda(t_0) \end{bmatrix} \notin Y \tag{19b}$$

where Y *is a linear subspace of* $\mathbb{R}^{2n}$*.*

Exponential dichotomy implies that $0 \leq j \leq 2n$ solution modes are decreasing and $(2n - j)$ solution modes are increasing as t grows. The j decreasing modes and $(2n - j)$ increasing modes are controlled to moderate size by the boundary conditions at t_0 and t_f, respectively. Exponential dichotomy is a necessary and sufficient condition for asymptotic stability of the Hamiltonian BVP.

Theorem 6. *Let the assumptions of Theorem 4 hold, then the Hamiltonian BVP has exponential dichotomy and can be decomposed into asymptotically stable solutions in forward and reverse time by the dichotomy transformation given as follows:*

$$\begin{bmatrix} z(t) \\ \lambda(t) \end{bmatrix} = \begin{bmatrix} I & I \\ P(t) & N(t) \end{bmatrix} \begin{bmatrix} \sigma(t) \\ \rho(t) \end{bmatrix}. \tag{20}$$

Proof. See Appendix A for proof.

Building upon Theorem 4, the dichotomy transformation decomposes the original Hamiltonian BVP into two independent problems, wherein the contracting and expanding dynamics are decoupled. These solution modes are pinned down by the prescribed initial and final conditions and are thus ensured to be asymptotically stable in their corresponding time directions. Due to exponential dichotomy, van Keulen [31] showed that these results also hold for $t_f \to \infty$,

and that path constraints can also be handled; since $(0,0) \in int(\mathcal{X} \times \mathcal{U})$, these constraints will not be active beyond a finite horizon. In addition, for numerical robustness, we can handle these as soft constraints with ℓ_1 or quadratic penalties as shown below in (36).

3. Formulation and Properties of Infinite Horizon NMPC

The previous section presents and analyzes the properties under which infinite horizon NMPC with the terminal segment is well-posed and robust; this applies to a wide variety of dynamic systems [30]. In this section we formulate our proposed NMPC approach that builds on these properties. While previous studies have considered the construction of terminal regions for NMPC [33, 34], few studies have considered infinite horizon concepts directly in NMPC implementations. Notable exceptions are [23, 35] which consider infinite horizons with the time transformation $\tau = tanh(\gamma t)$. However, these studies use the transformation for the entire time domain, consider only open loop stable systems and do not explore stability properties.

3.1. Derivation of Terminal Cost

We extend Problem (1) to the following NMPC subproblem solved at time t_k with plant state x_k:

$$V(x_k) = \min \quad (\sum_{l=0}^{N-1} \psi(z_l, v_l) + \Phi(z_N))\Delta t \tag{21a}$$

$$s.t. \quad z_{l+1} = F(z_l, v_l), z_0 = x_k \quad l = 0, \dots N-1 \tag{21b}$$

$$0 = \bar{F}(z_N, \bar{v}), z_N \in \mathcal{X} \tag{21c}$$

$$z_l \in \mathcal{X}, v_l \in \mathcal{U}, \quad l = 0, \dots N-1 \tag{21d}$$

with the desired steady state defined at $z_s = 0$, which follows from the exponential dichotomy property. In the terminal segment, the discrete dynamic model

(21c) typically stems from an index-1 DAE model, which can be simplified to $d\bar{z}/dt = f(\bar{z}, \bar{v})$. Here, the domain of the terminal segment in the horizon is $t \in [\bar{t}, \infty)$, where $\bar{t} = t_k + N\Delta t$, $(\bar{z}, \bar{v})$ are the states and controls, and

$$\bar{F}(z_N, \bar{v}) = z_N + \int_{\bar{t}}^{\infty} f(\bar{z}(t), \bar{v}(t))dt. \tag{22}$$

We determine the terminal cost $\Phi(z_N)\Delta t$ in (21) as an approximation to the infinite sum $\sum_{l=N}^{\infty} \psi(\bar{z}_l, \bar{v}_l)\Delta t$, multiplied by a safety factor $\beta > 1$. This allows calculation of $\Phi(z_N)$ from numerical quadrature of $\int_{\bar{t}}^{\infty} \psi(\bar{z}(t), \bar{v}(t))dt$, as described in Section 3.2, and leads to the following error bounds.

- First, we have:

$$\left| \int_{\bar{t}}^{\infty} \psi(\bar{z}(t), \bar{v}(t))dt - \sum_{l=N}^{\infty} \psi(\bar{z}_l, \bar{v}_l)\Delta t \right| \leq \bar{\epsilon}_1$$

  where $\bar{\epsilon}_1$ is the discretization error between the integral and the infinite sum of the stage costs.

- Second, the terminal cost $\Phi(z_N)$ uses a numerical approximation of $\int_{\bar{t}}^{\infty} \psi(\bar{z}(t), \bar{v}(t))dt$, with:

$$\left| \Phi(z_N) - \frac{\beta}{\Delta t} \int_{\bar{t}}^{\infty} \psi(\bar{z}(t), \bar{v}(t))dt \right| \leq \frac{\beta}{\Delta t}\bar{\epsilon}_2$$

  where $\bar{\epsilon}_2$ is the quadrature error. Substituting for the above integral leads to:

$$\left| \Phi(z_N) - \beta \sum_{l=N}^{\infty} \psi(\bar{z}_l, \bar{v}_l) \right| \leq \frac{\beta}{\Delta t}\epsilon_q \tag{23}$$

  where $\epsilon_q = \bar{\epsilon}_1 + \bar{\epsilon}_2$, and $\beta \geq 1$. Since the terminal cost incorporates a quadrature approximation, the additional parameter β allows $\Phi(z_N)$ to overestimate the infinite sum $\sum_{l=N}^{\infty} \psi(\bar{z}_l, \bar{v}_l)$.

3.2. Incorporating the Time Transformation into the Terminal Segment

From (22) and the transformation $\tau = tanh(\gamma(t - \bar{t}))$, where $\gamma > 0$ is a tuning parameter, we have the corresponding transformed equation:

$$\bar{F}(z_N, \bar{v}) - z_N = \int_{\bar{t}}^{\infty} f(\bar{z}(t), \bar{v}(t))dt = \int_0^1 f(\bar{z}(\tau), \bar{v}(\tau))/(\gamma(1-\tau^2))d\tau. \quad (24)$$

This corresponds directly to the time-transformed differential equation:

$$\frac{d\bar{z}}{d\tau} = f(\bar{z}(\tau), \bar{v}(\tau))/(\gamma(1-\tau^2)), \quad \bar{z}(0) = z_N \quad (25)$$

which we solve numerically over $\tau \in [0, 1]$ using $\bar{K}$-point orthogonal collocation with $\bar{N}$ finite elements, i.e.,

$$\gamma(1-\tau_{ik}^2)\sum_{j=0}^{\bar{K}} \dot{\ell}_j(\bar{\tau}_k)\bar{z}_{ij} = h_i f(\bar{z}_{ik}\bar{v}_{ik});\ \bar{z}_{1,0} = z_N \quad (26a)$$

$$\tau_{ik} = \tau_{i0} + \bar{\tau}_k h_i, \qquad i = 1, \bar{N},\ k = 1, \bar{K} \quad (26b)$$

$$\bar{z}_{i+1,0} = \sum_{j=0}^{\bar{K}} \ell_j(1)\bar{z}_{ij}, \qquad \tau_{i+1,0} = \tau_{i,0} + h_i \quad i = 1, \bar{N}-1 \quad (26c)$$

$$\tau_{1,0} = 0, \qquad \tau_{\bar{N},0} + h_{\bar{N}} = 1 \quad (26d)$$

where $\bar{\tau}_k \in (0, 1)$ are Gauss-Legendre roots, $\ell_j(\bar{\tau})$ are Lagrange basis polynomials and $h_i > 0$ are finite element lengths with $\sum_{i=1}^{\bar{N}} h_i = 1$. The time transformation $t \to \tau$ leads to the solution of an optimization problem with similar size and characteristics as Problem (1).

To determine the terminal cost numerically, we consider two options:

1. Riemann sum evaluated at collocation points used in (26):

$$\Phi(z_N)\Delta t = \beta \sum_{i=1}^{\bar{N}} \sum_{j=1}^{\bar{K}} \psi(\bar{z}_{ij}, \bar{v}_{ij})(t_{i,j} - t_{i,j-1}) \quad (27)$$

2. Gaussian quadrature obtained through $\bar{K}$-point orthogonal collocation with $\bar{N}$ finite elements. Here $\Phi(z_N) = \frac{\beta}{\Delta t}\varphi_f$, with:

$$\varphi_f = \int_{\bar{t}}^{\infty} \psi(\bar{z}(t), \bar{v}(t))dt = \int_0^1 \frac{\psi(\bar{z}(\tau), \bar{v}(\tau))}{\gamma(1-\tau^2)}d\tau$$

also satisfies the differential equation:

$$\frac{d\varphi}{d\tau} = \frac{\psi(z(\tau), v(\tau))}{\gamma(1-\tau^2)},\ \varphi(0) = 0 \text{ and } \varphi_f = \varphi(1) \tag{28}$$

which is solved numerically with the following collocation equations, analogous to (26):

$$\gamma(1-\tau_{ik}^2)\sum_{j=0}^{\bar{K}} \dot{\ell}_j(\bar{\tau}_k)\varphi_{ij} = h_i\psi(\bar{z}_{ik}\bar{v}_{ik});\ \varphi_{1,0} = 0 \tag{29a}$$

$$\tau_{ik} = \tau_{i0} + \bar{\tau}_k h_i, \qquad i = 1, \bar{N},\ k = 1, \bar{K} \tag{29b}$$

$$\varphi_{i+1,0} = \sum_{j=0}^{\bar{K}} \ell_j(1)\varphi_{ij}, \qquad \varphi_f = \sum_{j=0}^{\bar{K}} \ell_j(1)\varphi_{\bar{N}j} \tag{29c}$$

$$\tau_{i+1,0} = \tau_{i,0} + h_i \qquad i = 1, \bar{N}-1 \tag{29d}$$

$$\tau_{1,0} = 0, \qquad \tau_{\bar{N},0} + h_{\bar{N}} = 1 \tag{29e}$$

and $\Phi(z_N) = \frac{\beta}{\Delta t}\varphi_f$, which is applied in (21).

3.3. Nominal Stability of Infinite Horizon NMPC Controller

Problem (21) can be formulated to be recursively feasible. In shifting the solution at horizon t_k to the solution at horizon t_{k+1} we still satisfy the steady state constraints $z_{N|k} = z_{N|k+1} = z_s$, $v(\tau = 1)_{k+1} = v(\tau = 1)_k = v_s$. To show asymptotic stability, we also make the following assumptions.

Assumption 7. *The stage costs and terminal segment satisfy the following properties.*

- *The dynamic system is weakly controllable with*

$$0 \leq \psi(x,u) \leq \alpha_1(\|x - x_s\|) \text{ and } 0 \leq \Phi(x) \leq \alpha_2(\|x - x_s\|)$$

where $\alpha_1(\|x - x_s\|), \alpha_2(\|x - x_s\|)$ *are* $\mathcal{K}_\infty$ *functions of* $\|x - x_s\|$.

- *To preserve continuity for the shift into the terminal segment,* γ *is chosen so that the location of the first collocation point, e.g.,* $\tau_{1,1} \approx 0.1$ *in the terminal segment, satisfies* $tanh(\gamma \Delta t)$*, as illustrated in Figure 2.*

- *The quadrature error* ϵ_q *is sufficiently small so that the inequality*

$$\Phi(z_{N|k}) - \Phi(z_{N|k+1}) - \beta\psi(z_{N-1|k+1}, v_{N-1|k+1}) \geq -\varepsilon\psi(x_k, u_k) \qquad (30)$$

is satisfied with $\varepsilon \in [0, 1)$*, and*

$$\epsilon_q \leq \frac{\Delta t}{2\beta}\varepsilon\psi(x_k, u_k). \qquad (31)$$

Inequality 30 is derived by comparing (23) at k *and* $k+1$*, and 31 can be satisfied through an appropriate choice of collocation points in solving (25). This choice can even be made adaptively on-line.*

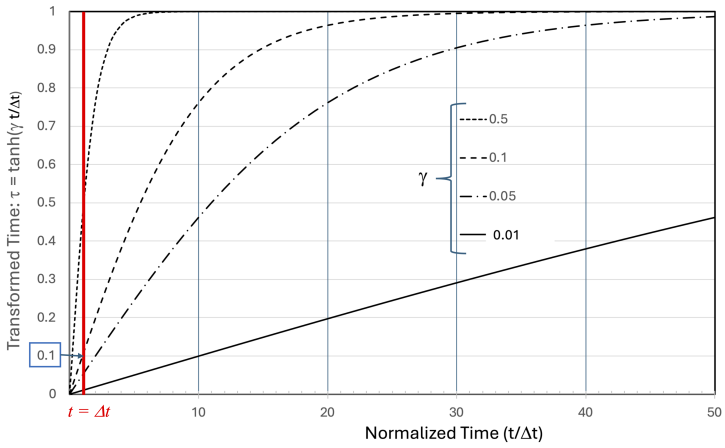

Figure 2: Selection of γ based on a sampling time Δt that corresponds to the first collocation point, $\tau_{1,1} = 0.1$. In this figure, $\gamma \approx 0.1$.

Under these assumptions, (30) leads to the following descent conditions for Problem (21):

$$\begin{aligned}
(V(x_k) - V(x_{k+1}))/\Delta t &= \sum_{l=0}^{N-1} \psi(z_{l|k}, v_{l|k}) - \sum_{l=0}^{N-1} \psi(z_{l|k+1}, v_{l|k+1}) + \Phi(z_{N|k}) - \Phi(z_{N|k+1}) \\
&\geq \psi(x_k, u_k) - \psi(z_{N-1|k+1}, v_{N-1|k+1}) \\
&\quad + \beta\psi(z_{N-1|k+1}, v_{N-1|k+1}) - \varepsilon\psi(x_k, u_k) \\
&\geq \psi(x_k, u_k) + (\beta - 1)\psi(z_{N-1|k+1}, v_{N-1|k+1}) - \varepsilon\psi(x_k, u_k) \\
&\geq (1 - \varepsilon)\psi(x_k, u_k) \qquad (32)
\end{aligned}$$

which follows from $\beta \geq 1$ and $\psi(z, v) \geq 0$. Summing (32) over k leads to:

$$V(x_0) \geq \sum_{k=0}^{\infty} [V(x_k, u_k) - V(x_{k+1}, u_{k+1})] \geq (1 - \varepsilon) \sum_{k=0}^{\infty} \psi(x_k, u_k))\Delta t \qquad (33)$$

which implies

$$\lim_{k \to \infty} \psi(x_k, u_k) = 0. \qquad (34)$$

These relations prove the following theorem.

Theorem 8. *Let (31) be satisfied for some* $\varepsilon \in [0, 1)$ *and UCC and Assumptions 7 hold, then the infinite horizon NMPC is asymptotically stable with* $x_k \to 0$ *and* $u_k \to 0$.

Finally, from the definition of the terminal cost $\Phi(z_N)$, we note that $\beta \geq 1$ is essential for stability. To see this, let $\beta < 1$ and from (32)-(33) we obtain

$$V(x_0) \geq \sum_{k=0}^{\infty} [(1-\varepsilon)\psi(x_k, u_k) - (1-\beta)\psi(z_{N-1|k+1}, v_{N-1|k+1})]\Delta t$$

and

$$\lim_{k\to\infty} [(1-\varepsilon)\psi(x_k, u_k) - (1-\beta)\psi(z_{N-1|k+1}, v_{N-1|k+1})] \to 0,$$

but not $\lim_{k\to\infty} \psi(x_k, u_k) \to 0$. As a result we are unable to show that NMPC is asymptotically stable with $\beta < 1$.

3.4. Robust Stability of Infinite Horizon NMPC

Robustness of NMPC requires the controller to operate in the presence of bounded model uncertainty and unmeasured disturbances, such that the sequence of plant states x_k are ensured to attract to a bounded neighborhood of the set-point. Here we extend the asymptotic stability property from Theorem 8 to input-to-state stability (ISS), by establishing a uniform continuity property for Problem (21).

We represent the feedback control law derived from solving (21) as $u_k = \kappa(x_k)$ and define the plant model as $\hat{F}_\kappa(x, w) := \hat{F}(x, \kappa(x), w)$, with w as the uncertain disturbance that accounts for the plant-model mismatch and $\hat{F}_\kappa(x, 0) = F(x, \kappa(x))$. The plant model is assumed to be uniformly continuous in w such that there exists a $\mathcal{K}$ function α_w with $\left|\hat{F}_\kappa(x, w) - \hat{F}_\kappa(x, w')\right| \leq$

$\alpha_w(|w-w'|)$. Since problem (21) admits a Lyapunov function, we have

$$\begin{aligned} V\left(\hat{F}_\kappa(x,w)\right) - V(x) &= V\left(\hat{F}_\kappa(x,w)\right) - V\left(\hat{F}_\kappa(x,0)\right) + V\left(\hat{F}_\kappa(x,0)\right) - V(x) \\ &\leq \left| V\left(\hat{F}_\kappa(x,w)\right) - V\left(\hat{F}_\kappa(x,0)\right)\right| - \alpha_3(|x|) \end{aligned} \tag{35}$$

where (35) follows from (32) and $\alpha_3(|x|)$ is a $\mathcal{K}_\infty$ function of $|x|$.

Using (35), input-to-state stability for the infinite horizon controller can be proved if we can show that $V(x)$ from (21) is uniformly continuous in w. The conditions for this property are detailed in Appendix B and are summarized below.

First, we consider the reformulation of (21) similar to the one proposed in [20], given at time t_k by:

$$V(\hat{F}_\kappa(x_{k-1},w)) = \min \quad \left(\sum_{l=0}^{N-1}\psi(z_l,v_l) + \Phi(z_N)\right)\Delta t + \mu\, e^T\left(\hat{\varepsilon} + \sum_{l=0}^{N}\left(\varepsilon_l^{up} + \varepsilon_l^{lo}\right)\right) \tag{36a}$$

$$s.t. \quad z_{l+1} = F(z_l,v_l),\ l=0,\dots N-1 \tag{36b}$$

$$z_e = \bar{F}(z_N,\bar{v}) \tag{36c}$$

$$z_e + \hat{z} = z_s,\ z_0 = \hat{F}_\kappa(x_{k-1},w) \tag{36d}$$

$$z^{lo} - \varepsilon_l^{lo} \leq z_l \leq z^{up} + \varepsilon_l^{up},\ l=0,\dots N \tag{36e}$$

$$z^{lo} \leq z_e \leq z^{up} \tag{36f}$$

$$-\hat{\varepsilon} \leq \hat{z} \leq \hat{\varepsilon} \tag{36g}$$

$$\bar{v}, v_l \in \mathcal{U},\ l=0,\dots N-1 \tag{36h}$$

$$\hat{\varepsilon}, \varepsilon_l^{up}, \varepsilon_l^{lo} \geq 0. \tag{36i}$$

where the state and control sets $\mathcal{X}$, $\mathcal{U}$ are represented by simple upper and lower bounds and $e^T = [1,1,\dots,1]$. In addition, we introduce the variable

$\hat{z} \in [-\hat{\varepsilon}, \hat{\varepsilon}]$ to allow for a relaxation of the steady-state endpoint constraint, and to accommodate the disturbance w. Correspondingly, $\varepsilon_l^{up}, \varepsilon_l^{lo}$ and $\hat{\varepsilon}$, are nonnegative slack variables and $\mu > 0$ is a penalty parameter. By selecting $\mu > \bar{\mu}$, the max-norm of the multipliers at the optimum of problem (21). If $\bar{\mu}$ is finite, then the slack variables will be driven to zero in the soft-constrained problem and the solution of (36) is identical to the solution of (21).

Next, the conditions under which the solution of (36) is Lipschitz continuous (and thereby uniformly continuous) with respect to perturbations w are the following.

- Mangasarian-Fromovitz constraint qualification (MFCQ) (Definition 13)
- Generalized Strong Second-order Sufficient Condition (GSSOSC) (Definition 14)

at the optimal solution characterized by the Karush-Kuhn-Tucker (KKT) point (Definition 12) [20]. In Appendix B, we show that (36) satisfies both MFCQ and GSSOSC at the optimal solution. Thus, the solution of (36) is Lipschitz continuous with respect to w.

Finally, combining the continuity property of $V(x)$ with respect to x and w, the descent condition in (35) now becomes

$$V\left(\hat{F}_\kappa\left(x,w\right)\right) - V\left(x\right) \leq \alpha_V\left(\left|\hat{F}_\kappa\left(x,w\right) - \hat{F}_\kappa\left(x,0\right)\right|\right) - \alpha_3\left(|x|\right) \tag{37a}$$

$$\leq \alpha_V \circ \alpha_w\left(|w|\right) - \alpha_3\left(|x|\right) \tag{37b}$$

where $\alpha_V(\xi)$ is a $\mathcal{K}_\infty$ function of $\xi \in \mathbb{R}_{\geq 0}$. As shown in Definitions 9 and 10 in Appendix B, this implies that $V\left(\cdot\right)$ is an ISS-Lyapunov function and the resulting system is input-to-state stable. Consequently, the following theorem holds.

Theorem 9. *Let the assumptions for Theorem 8 hold, then MFCQ and GSSOC are satisfied at KKT points of Problem (36) and the corresponding infinite-horizon NMPC is input-to-state stable.*

4. Case Study Demonstrations of Infinite Horizon NMPC

This section presents case studies for three NMPC examples: a jacketed continuous stirred tank reactor (CSTR), an inverted pendulum, and a rigorous binary distillation column, in order to demonstrate the performance of the proposed infinite horizon NMPC formulation.

For all three examples, the dynamic models were generated using Pyomo [36], and all time points were initialized with steady state values before the initial solve. According to standard NMPC practice, the controller solves the optimization problem (36) at time k. Then the plant model is simulated by taking $u_k = v_0$ from this solution to obtain the plant state variables at time $k+1$. Then $k := k+1$, $z_0 := x_k$ and problem (36) is solved again. This approach is used for the case studies in this section. For each case study, problem size and solution time per horizon are recorded. All numerical results were obtained on an AMD Ryzen 5 7600X 6-Core, 12-Thread processor.

A note on the plots – in the CSTR and inverted pendulum cases, only data at the finite elements are plotted, not at the collocation points within each finite element. In the distillation case, all plant data are plotted, including the data with finite elements, which is why piecewise constant behavior is more clearly observed for the manipulated variables. (Recall that the manipulated variables are decisions made by the controller that only take effect at each plant sampling time, but the state variables are continuously changing, and their behavior is approximated by collocation points.) While piecewise constant input behavior is part of all models, this can only be discerned in the distillation plots.

4.1. Non-isothermal CSTR

We first consider the non-isothermal CSTR (Example 13-3 in [37]), with the following DAEs for the reaction $A + B \to C$ in the presence of component M:

$$\frac{dC_i}{dt} = \frac{\nu_0}{V}(C_{i0} - C_i) + s_i k C_A,\ k = 1.696 \times 10^{13} \exp\left(\frac{-18012}{1.987T}\right) \tag{38a}$$

$$s = (-1, -1, 1, 0), N_i = C_i V,\ \forall i \in \{A, B, C, M\} \tag{38b}$$

$$\frac{dT}{dt} = \frac{Q_g - (Q_{r1} + Q_{r2})}{N_{C_p}}, \tag{38c}$$

$$\theta_{C_p} = 35 + \frac{18F_{B0}}{F_{A0}} + \frac{19.5F_{M0}}{F_{A0}},\ v_0 = \frac{F_{A0}}{14.8} + \frac{F_{B0}}{55.3} + \frac{F_{M0}}{24.7} \tag{38d}$$

$$T_{A2} = T - \left(\left(T - T_{A1} \exp\left(-\frac{UA}{C_{p,W} \cdot m_c}\right)\right)\right),\ C_{i0} = \frac{F_{i0}}{v_0}\ \ \forall i \in \{A, B, M\} \tag{38e}$$

$$Q_{r2} = m_c \cdot C_{p,W} \cdot (T_{A2} - T_{A1}),\ Q_{r1} = F_{A0} \cdot \theta_{C_p} \cdot (T - T_0) \tag{38f}$$

$$Q_g = -kC_A \cdot V \cdot \Delta H_r,\ N_{C_p} = 35N_A + 18N_B + 46N_C + 19.5N_M \tag{38g}$$

with $F_{A0} \geq 100$, $m_c \leq 250$ as manipulated variables, and T, C_c as controlled variables, where F_{A0} is the inlet molar flow rate of component A, m_c is the mass flow of cooling water through the CSTR jacket, T is the CSTR bulk temperature, and C_c is the concentration of product C in the CSTR. V, F_{B0}, F_{M0}, UA, $C_{p,W}$, T_{A1}, T_0, and ΔH_r are constants reported in [37].

After discretization over the time domain, an algebraic system is obtained and an optimization problem can be formulated according to (36), with the stage cost defined as

$$\psi(z_l, v_l) = (C_{c,l} - C_{c,sp})^2 + 10^{-2}(T_l - T_{sp})^2 + 10^{-3}(F_{A0,l} - F_{A0,ss})^2 + 10^{-3}(m_{c,l} - m_{c,ss})^2 \tag{39}$$

4.1.1. Finite/Infinite Horizon Comparison

We compare the infinite horizon NMPC formulation in (36) with the baseline NMPC formulation without terminal conditions, shown in (5). Here, the baseline NMPC has $N = 2$ and $N = 20$, while infinite horizon NMPC has $N = 2$ Each controller uses 5 collocation points in each element, the sampling time is 0.0025 hours (9 seconds) and $t_h = \Delta t \cdot N$ where t_h is the horizon time, Δt is the sampling time. The terminal segment for infinite horizon NMPC has $\bar{N} = 3$ finite elements and 5 Legendre collocation points with $\beta = 1.2$ and $\gamma = 6$.

Figures 3 - 6 show C_c and T (controlled variables), and F_{A0} and m_c (manipulated variables) vs. time for the three controllers: Also plotted are the setpoint values for the two controlled variables.

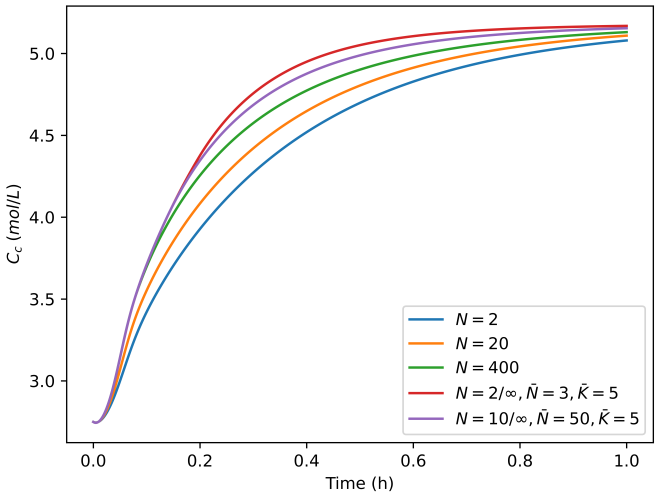

Figure 3: Dynamic Product Concentration (CV) for Finite Horizon and Infinite Horizon Cases

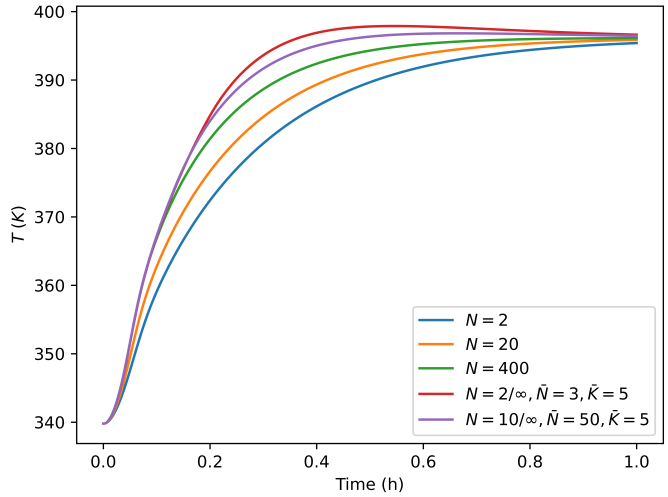

Figure 4: Dynamic Reactor Temperature (CV) for Finite Horizon and Infinite Horizon Cases

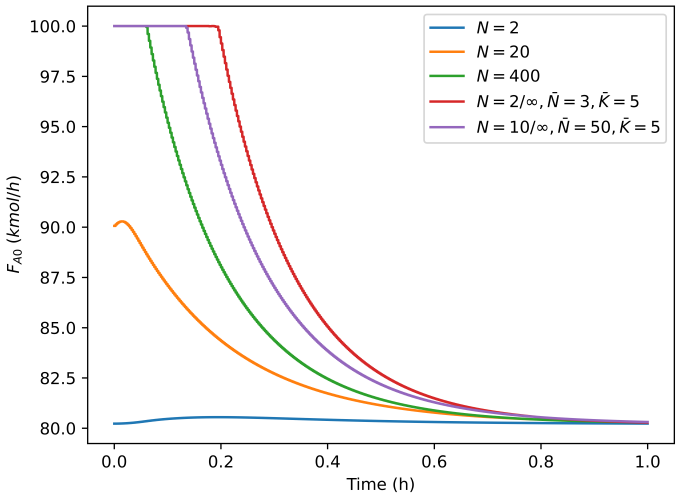

Figure 5: Dynamic Reactant Inlet Flow (MV) for Finite Horizon and Infinite Horizon Cases

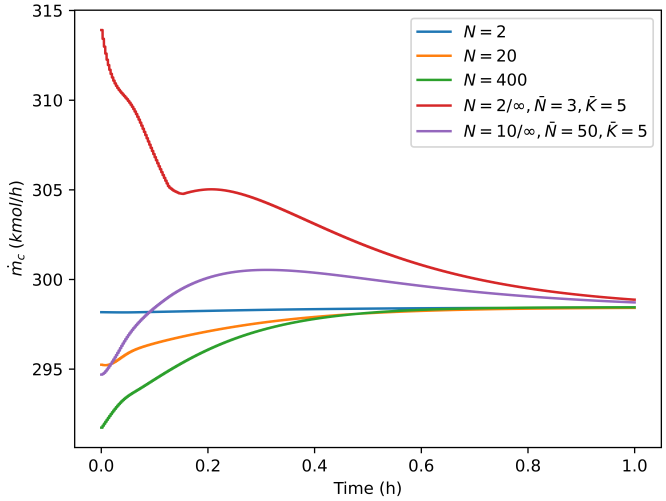

Figure 6: Dynamic Coolant Flow (MV) for Finite Horizon and Infinite Horizon Cases

We observe from the above plots that the infinite horizon NMPC approaches the steady state at a faster rate than with the baseline controllers with $N = 2, 20$ and 400. Moreover, the performance of these controllers can be quantified as cumulative error by integrating the stage cost over the total time (1 hour). The number of variables, equality constraints, simulation time per horizon (CPU s) for each case, and cumulative error are shown in Table 1. Also, note that the infinite horizon NMPC with $N = 2$ is 2.6 times faster than baseline NMPC with $N = 20$. To observe limiting behavior as $N \to \infty$, we consider the baseline case for $N = 400$ as well as infinite horizon NMPC with $N = 10$. Here we note similar error reductions with increasing N and refinement of the terminal costs. On the other hand, since the terminal cost in infinite horizon NMPC is only an approximation to the infinite sum of stage costs (especially with $\beta > 1$), the infinite horizon NMPC profiles may differ slightly from baseline NMPC with large N.

	Variables	Constraints	CPU s	Error
Baseline, $N = 2$	120	116	0.0046	4.818
Baseline, $N = 20$	1200	1160	0.0316	4.131
Baseline, $N = 400$	24000	23200	0.6407	3.837
∞ horizon, $N = 2$	355	319	0.0119	4.154
∞ horizon, $N = 10$	3767	3565	0.0994	3.9452

Table 1: NMPC problem sizes, CPU times, and performance for CSTR example

4.1.2. Tuning Parameter Comparison

For further analysis of infinite horizon NMPC, we examine the effect of the tuning parameters β and γ on the model output. Recall that $\beta > 1$ is needed to ensure an over-approximation of the terminal cost, which guarantees stability as long as condition (31) is satisfied, and we also note that if $\beta = 0$, there is no penalty for setpoint deviation in the terminal infinite region. However, we still have an endpoint constraint for the controller, driving the system to the setpoints. Profiles for the infinite horizon cases (with $N = 2$), $\beta = 1.2$ with $\gamma = 6$, $\gamma = 4000$ and $\gamma = 0.0004$, $\beta = 10$ with $\gamma = 6$, and $\beta = 0$ with $\gamma = 6$ are included for analysis.

Plotted together, we have Figures 7-10 and note the following observations.

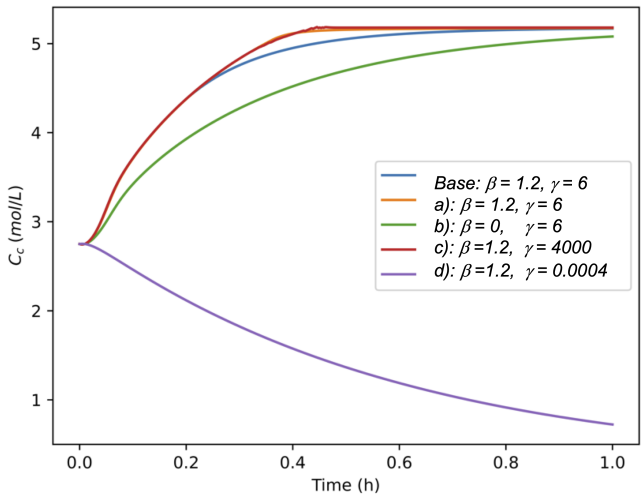

Figure 7: Dynamic Product Concentration (CV) for Parameter Tuning Cases

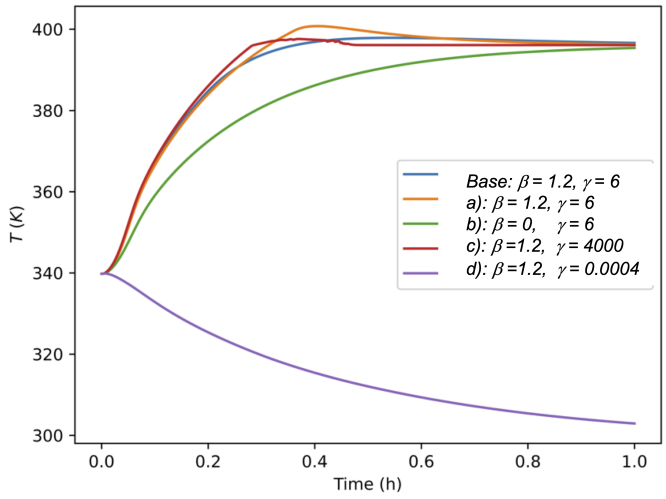

Figure 8: Dynamic Reactor Temperature (CV) for Parameter Tuning Cases

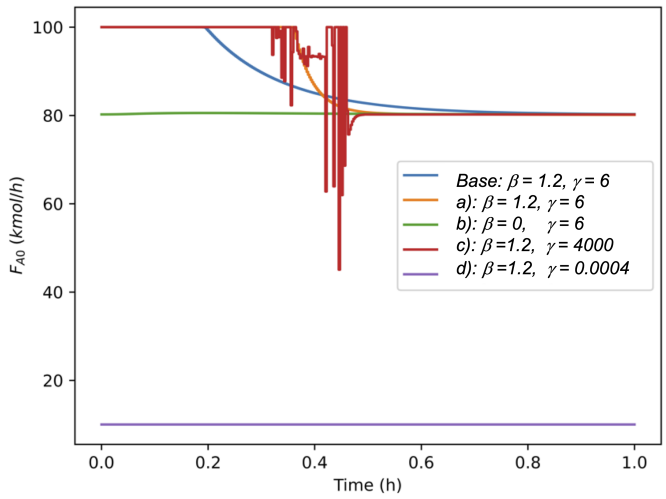

Figure 9: Dynamic Reactant Inlet Flow (MV) for Parameter Tuning Cases

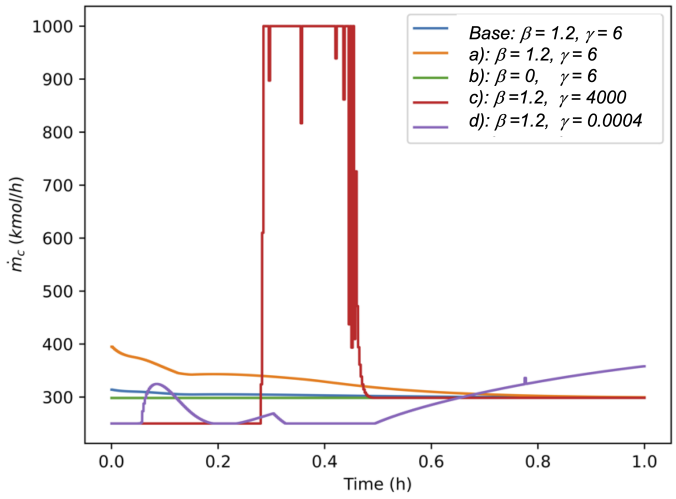

Figure 10: Dynamic Coolant Flow (MV) for Parameter Tuning Cases

a) Increasing $\beta > 1$ produces plots with weaker setpoint convergence than with

the base value. A higher β value overestimates the value of the stage costs in the terminal segment, leading to satisfaction of condition 30, but performing sub-optimally.

b) Elimination of the terminal cost ($\beta = 0$) makes the behavior of the infinite horizon NMPC revert to baseline NMPC. Note that the only difference in the two formulations is the presence of endpoint constraints on the control variables at the end of the terminal segment. The state profiles for $\beta = 0$ therefore trend more closely to the baseline NMPC profiles in Figures 3 and 4.

c) Increasing the value of γ to 4000 accelerates the time decay in the τ domain, so that state derivatives with respect to τ are smaller for larger values of γ, according to

$$\frac{dz}{d\tau} = \frac{f(z,t)}{\gamma(1-\tau^2)}.$$

This means the controller approaches the steady state earlier in the transformed domain, and because of the endpoint constraints, the controller may be more limited in its control actions by the dynamics of the system. In Figures 9 and 10 we observe significant numerical oscillations, and offline calculations of ε in condition 30 show consistent violations, as expected when γ is too large.

d) Decreasing the value of γ to 0.0004 has the opposite effect on relative magnitudes of differential variable values. We observe in Figures 7 - 10 that with small γ the controller does not drive the system to setpoints. This is not due to numerical oscillation, but as a result of violations of condition 30.

In general, our observations show that a selection of γ based on the first collocation point according to Figure 2 provides satisfactory controller performance.

4.1.3. Alternate Terminal Cost Formulation for Terminal Infinite Horizon Segment

We now compare the collocation formulation for terminal cost with the Riemann sum outlined in (27) with $N = 2$, $\beta = 1.2$ and $\gamma = 6$ unless otherwise noted. The resulting plots from this formulation are shown in Figures 11 - 14, with different numbers of finite elements in the infinite region for each. In general, the Riemann sum formulation is less accurate, but simpler to implement, approximation of the infinite sum, with only minor differences observed in NMPC performance. Additionally, as the number of finite elements in both the finite and infinite regions increase, the controller approaches $N = 400$ performance. This is most clearly observed in Figures 13 and 14.

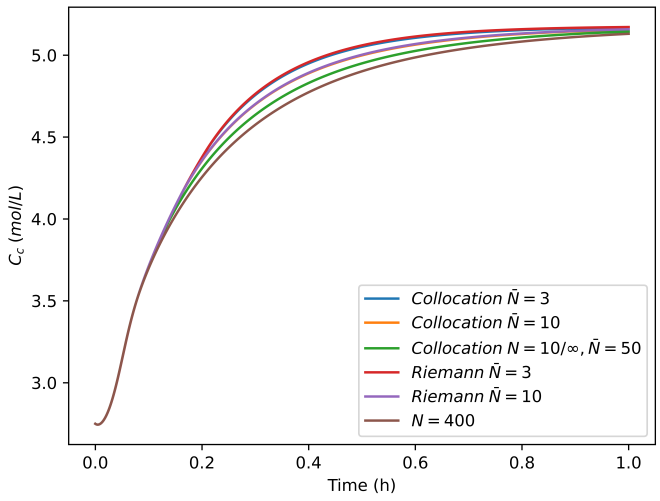

Figure 11: Dynamic Product Concentration (CV) for Terminal Cost Cases

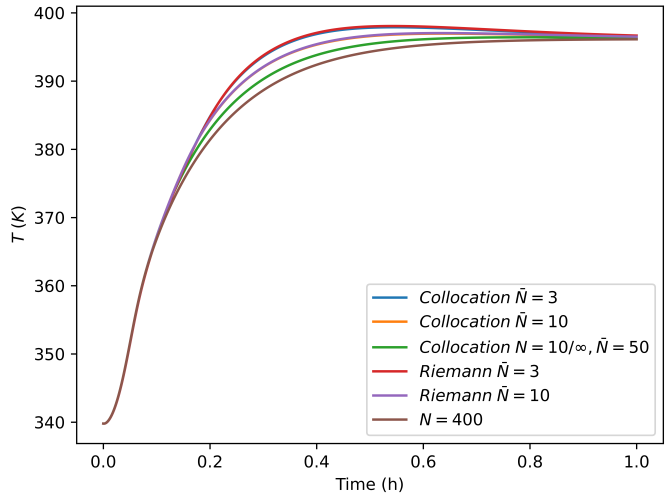

Figure 12: Dynamic Reactor Temperature (CV) for Terminal Cost Cases

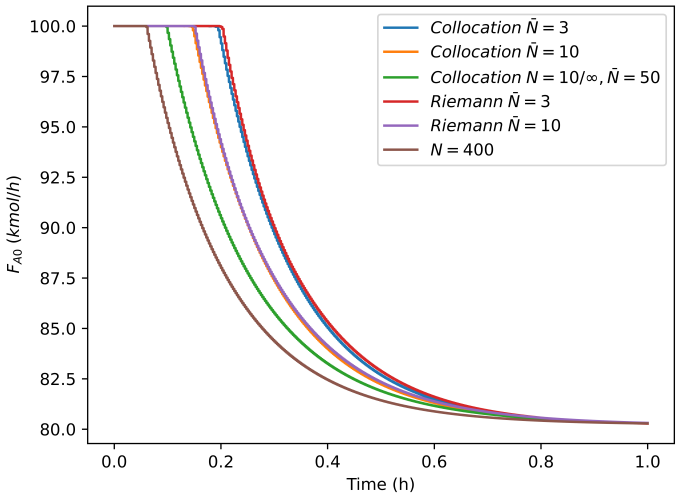

Figure 13: Dynamic Reactant Inlet Flow (MV) for Terminal Cost Cases

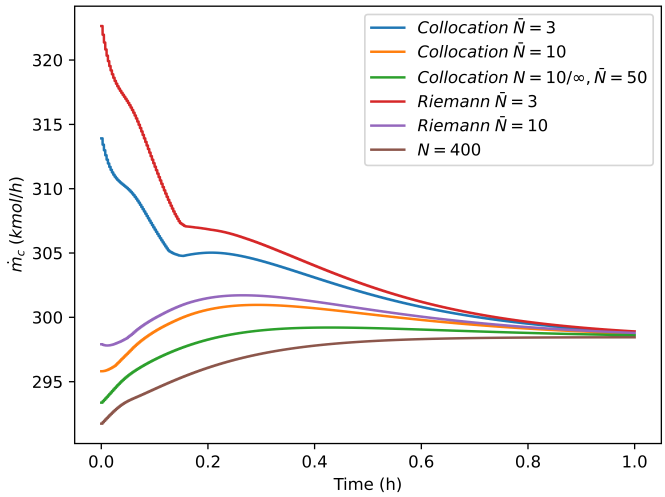

Figure 14: Dynamic Coolant Flow (MV) for Terminal Cost Cases

4.2. Inverted Pendulum

The inverted pendulum problem is a classic control example demonstrating open loop instability, a challenge the infinite horizon approximation overcomes by constraining the final values of the control variables to their setpoints. Physically, this system is a cart to which forces can be applied horizontally in either direction in one dimension. On top of the cart is a hinged, massless rod, with a point mass at its end. Here, the rod angle perpendicular to the ground is the controlled variable, while the applied force is the manipulated variable. In this study we only control the rod angle, though we include a terminal condition for the position x as well. The differential equations shown below are taken from

[38].

$$\frac{d^2x}{dt^2}\left(m_p\cos^2(\theta)-(1+k)(m_p+m_c)\right)$$
$$=m_pg\sin(\theta)\cos(\theta)-(1+k)\left(F+m_pl\left(\frac{d\theta}{dt}\right)^2\sin(\theta)-\mu_c\frac{dx}{dt}\right) \quad (40a)$$
$$\frac{d^2\theta}{dt^2}\left((1+k)(m_p+m_c)l-m_pl\cos^2(\theta)\right)$$
$$=(m_p+m_c)g\sin(\theta)-\cos(\theta)\left(F+m_pl\left(\frac{d\theta}{dt}\right)\sin(\theta)-\mu_c\frac{dx}{dt}\right) \quad (40b)$$

The corresponding optimization problem is formulated according to (36), with the stage cost defined as

$$\psi(z_l,v_l)=(\theta_l-\theta_{sp})^2+(x-x_{sp})^2+(F_l-F_{ss})^2. \quad (41)$$

Initial values of zero for position, velocity, and angular velocity, and a starting angle of the pendulum $\theta(0)=10^\circ$ were used to initialize the model. For infinite horizon NMPC, $\beta=1.2$ and $\gamma=0.0375$ were used. The time was discretized with varying numbers of finite elements (corresponding to horizon length), 5 collocation points over each finite element and a sampling time of $\Delta t=0.2s$. Figures 15-17 present the baseline controller results with $N=5$ and $N=50$ steps and infinite horizon NMPC with $N=5$ and a terminal segment with $\bar{N}=6$ finite elements and $\bar{K}=5$ collocation points; these display plots of the manipulated variable (force), and the controlled variables (position, pendulum angle) with respect to time.

As seen in Figs. 15 - 17, the baseline NMPC with $N=5$ does not reach steady state in the time interval, while baseline NMPC with $N=50$ and infinite horizon NMPC quickly converge to zero setpoints. The number of variables and constraints, and simulation times per horizon for each case are given in Table 2.

	Variables	Equality Constraints	Simulation Time/Horizon (CPU s)
Baseline, $N = 5$	225	220	0.0077
Baseline, $N = 50$	2250	2200	0.0512
∞ horizon, $N = 5$	590	554	0.0171

Table 2: NMPC problem sizes and CPU times for inverted pendulum example

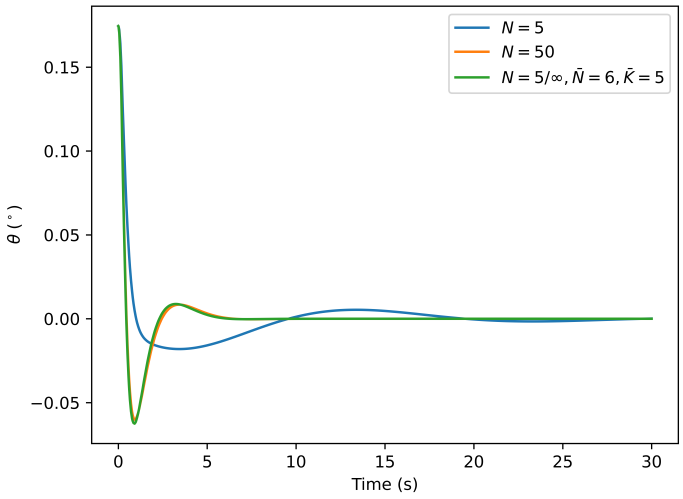

Figure 15: Inverted Pendulum Cart Position (State Variable) for Finite and Infinite Horizon Cases

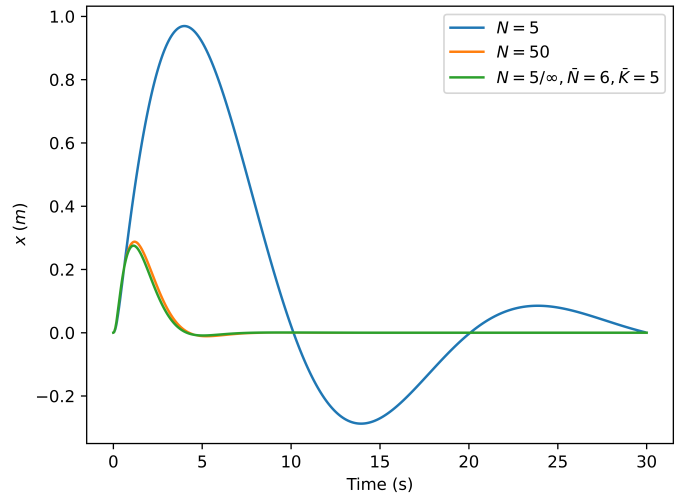

Figure 16: Inverted Pendulum Angle (CV) for Finite and Infinite Horizon Cases

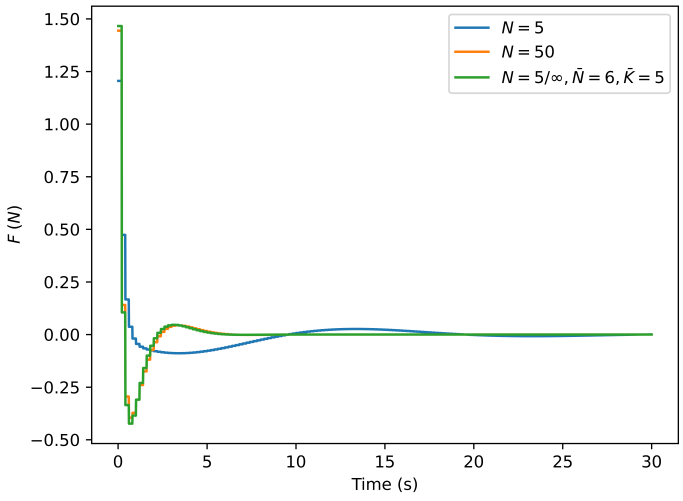

Figure 17: Inverted Pendulum Cart Force (MV) for Finite and Infinite Horizon Cases

4.3. Binary Distillation

A binary distillation column model was formulated with manipulated variables of reflux ratio and reboiler heat duty. The controlled variables are the composition of the light component in the distillate (x_{top}) and a bottom column temperature (T_{29}). The NMPC problem was considered with and without disturbance. Here we use a detailed DAE model based on the MESH equations presented in [39].

The NMPC optimization problem is formulated according to (36), with the stage cost defined as:

$$\psi(z_l, v_l) = 10^4(x_{top,l} - x_{top,sp})^2 + 10^3(T_{29,l} - T_{29,sp})^2. \tag{42}$$

Infinite horizon NMPC has $N = 2$, $\bar{N} = 1$. Baseline and infinite horizon NMPC use 5 collocation points in each finite element, with a sampling time of 10 min. The infinite horizon terminal cost approximation is formulated as a Riemann sum with 5 steps (at the collocation points) according to 27. For this model, $\beta = 1.2$, $\Delta t = 0.167h$ and $\gamma = 0.3$ based on $\tau_{1,1} = tanh(\gamma \Delta t)$. Figures 18-25 compare infinite horizon NMPC without and with disturbances against baseline NMPC with $N = 3$ and $N = 20$.

4.3.1. Binary Distillation Without Disturbance

Figures 18-21 compare the finite horizon approach with the infinite horizon formulation. From the resulting plots of each of the manipulated variables and controlled variables for the three controllers, we observe in Figure 18 that baseline NMPC with $N = 3$ cannot reach the setpoint for x_{top}. This horizon is inadequate because of its inability to predict the long-term behavior of the system. On the other hand, baseline NMPC with $N = 20$ and infinite horizon NMPC both drive the controlled variables to their setpoints, with slightly faster

performance for the latter approach.

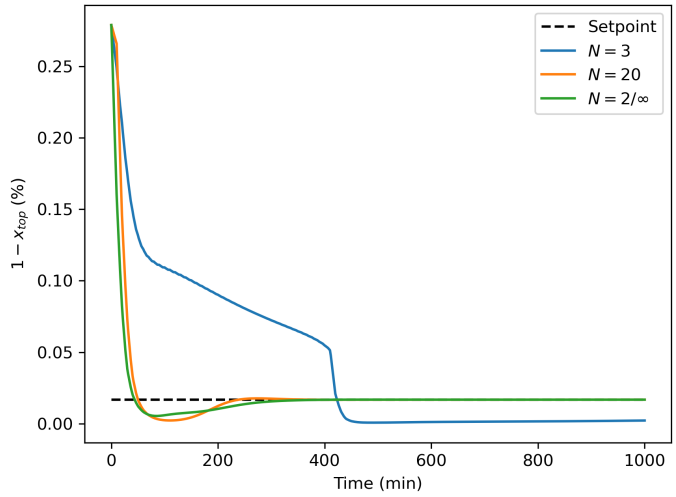

Figure 18: 1 - Top Product Mole Concentration (CV) for Finite and Infinite Horizon Cases

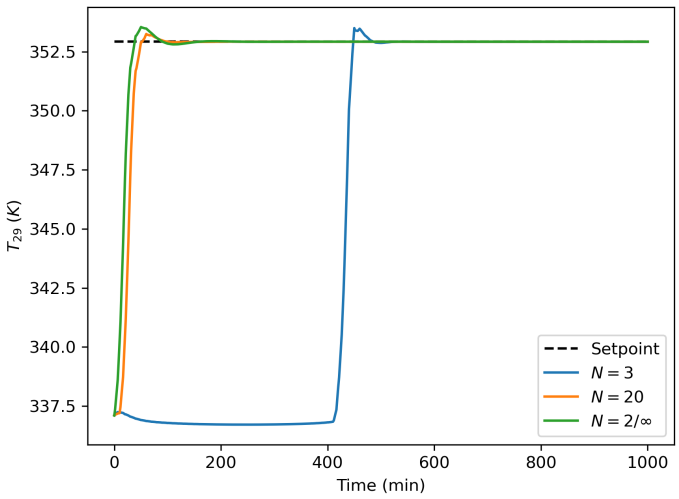

Figure 19: Tray 29 Temperature (CV) for Finite and Infinite Horizon Cases

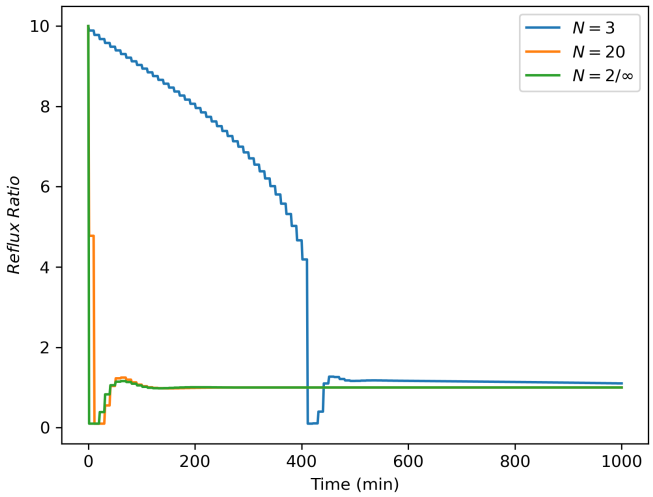

Figure 20: Reflux Ratio (MV) for Finite and Infinite Horizon Cases

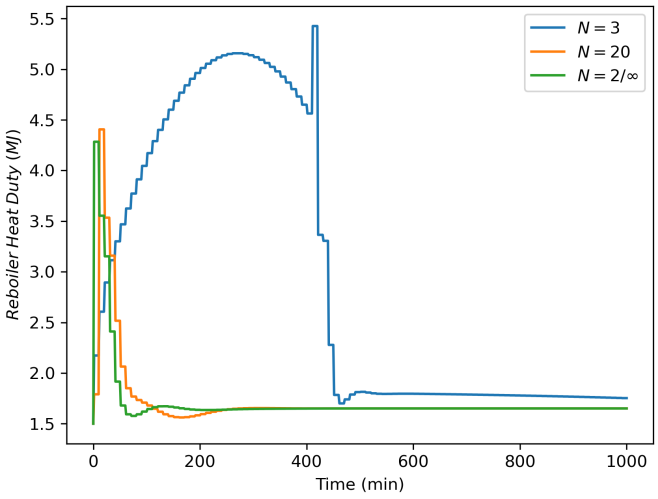

Figure 21: Reboiler Heat Duty (MV) for Finite and Infinite Horizon Cases

4.3.2. Binary Distillation With Disturbance

Disturbances are introduced from nominal feed mole fraction values; these are normally distributed with a relative standard deviation of 9%. For reproducibility, a random number generator determines the disturbed values, using the iteration number as a seed. This leads to the results in Figures 22-25. In Figures 22 and 23 we observe again that the baseline NMPC with $N = 3$ takes longer to approach the setpoint while both infinite horizon NMPC and baseline NMPC with $N = 20$ quickly drive and maintain their plants close to their setpoints.

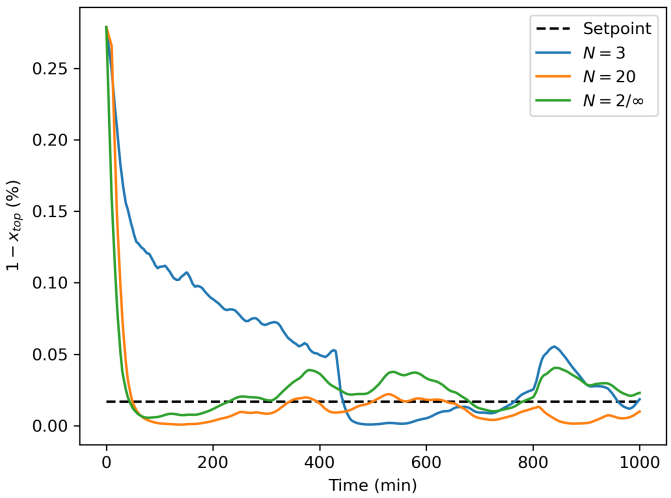

Figure 22: 1 - Top Product Mole Concentration for Finite and Infinite Horizon Cases with Disturbance

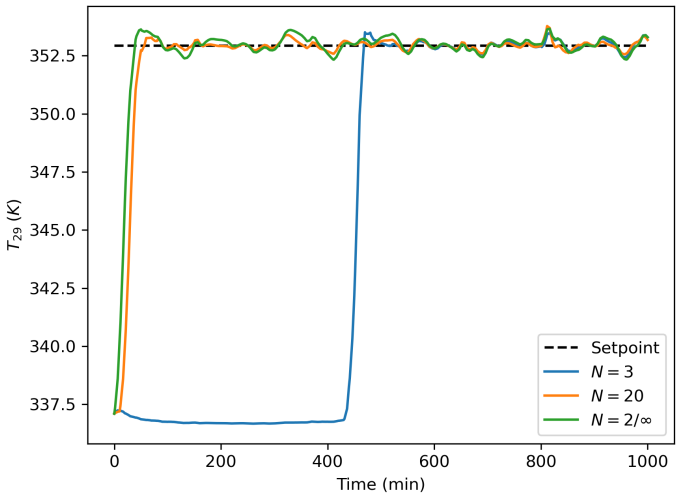

Figure 23: Tray 29 Temperature (CV) for Finite and Infinite Horizon Cases with Disturbance

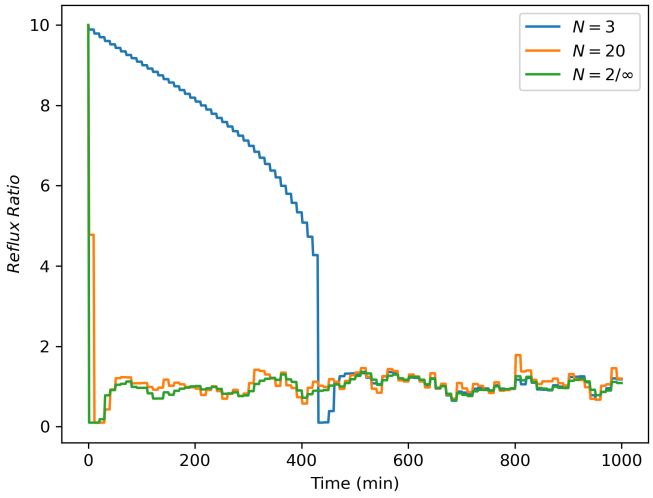

Figure 24: Reflux Ratio (MV) For Finite and Infinite Horizon Cases with Disturbance

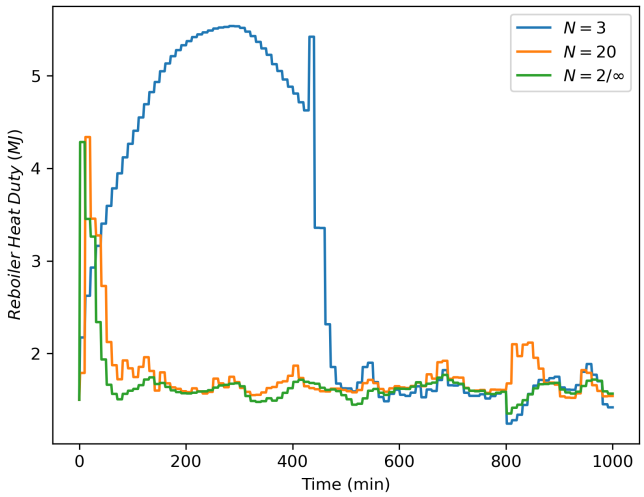

Figure 25: Reboiler Heat Duty (MV) for Finite and Infinite Horizon Cases with Disturbance

Finally, the NLP problem sizes (number of variables, equality constraints, and inequality constraints) for each case are shown in Table 3, and average run times per horizon are shown in Table 4 for each case, with and without disturbances. We note that run times for infinite horizon NMPC are similar to the (unsuccessful) $N = 3$ baseline NMPC and over an order of magnitude faster than for the (successful) $N = 20$ baseline NMPC.

	Variables	Equality Constraints	Inequality Constraints
Baseline, $N = 3$	3284	3278	1260
Baseline, $N = 20$	20471	20431	7686
∞ horizon, $N = 2$	3284	3274	1260

Table 3: NMPC problem sizes for binary distillation example

	Without Disturbance	With Disturbance
Baseline, $N = 3$	1.3164	1.3429
Baseline, $N = 20$	17.8924	22.3808
∞ horizon, $N = 2$	1.2855	1.5985

Table 4: NMPC run times (CPU s/horizon) for binary distillation example

5. Conclusions and Future Directions

Formulated and solved as nonlinear programs, NMPC strategies enjoy asymptotic and robust stability properties only if their horizon lengths are sufficient to satisfy endpoint or terminal region constraints. On the other hand, stability guarantees for infinite horizon NMPC are well known, but their practical implementation generally leads to intractable optimization problems. This study develops an alternate infinite horizon NMPC strategy that overcomes this computational barrier. Here, an infinite-horizon time transformation is appended as the terminal segment within a moving horizon NMPC framework. This infinite segment is formulated as an optimal control problem in transformed time that ensures satisfaction of the (steady state) setpoint. The resulting NMPC approach is recursively feasible and inherits the stability guarantees of infinite horizon NMPC.

Derived and analyzed as an extended boundary value problem, the terminal segment satisfies an exponential dichotomy property that pins down unstable modes, and therefore extends to open-loop unstable dynamic systems. The problem formulation is solved directly with orthogonal collocation on finite elements.

For the proposed approach, both asymptotic and robust stability properties are analyzed under reasonable assumptions, along with sufficient conditions on the approximation error for the terminal segment. In addition, efficacy and robustness of this approach are demonstrated on two process examples, as well

as an unstable inverted pendulum problem.

Future work will extend the proposed approach to economic NMPC over infinite horizons and will consider larger and more challenging applications in dynamic real-time optimization and dynamic scheduling with rolling horizons.

Appendix A.

The proofs for Theorem 4 and Theorem 6 are adapted from [29, 31] and summarized in this appendix, as they provide insight into how the BVP pins down the unstable modes so that stable solutions can be ensured.

Proof of Theorem 4. Conditions for existence and uniqueness of the symmetric positive definite root $P(t)$ of the Riccati differential equation subject to a symmetric positive semidefinite condition $K = \Gamma$ at the endpoint $t = t_f$ are well-known; see [32] for the stability proof. Here we derive the associated property of the symmetric negative definite root $N(t)$. Consider a distinct linear optimal control problem that minimizes:

$$\hat{J} = \frac{1}{2}\int_{t_0}^{t_f} \left[\hat{z}^T(t')\, Q(t_0 + t_f - t')\, \hat{z}(t') + \hat{v}^T(t')\, R(t_0 + t_f - t')\, \hat{v}(t')\right] dt' \tag{A.1}$$

subject to

$$\dot{\hat{z}}(t') = -A(t_0 + t_f - t')\, \hat{z}(t') - B(t_0 + t_f - t')\, \hat{v}(t') \tag{A.2}$$

with $\hat{z}$ specified at $t' = t_0$. The relevant Riccati differential equation

$$\begin{aligned}\dot{\hat{K}}(t') = {} & A^T(t_0 + t_f - t')\, \hat{K}(t') + \hat{K}(t')\, A(t_0 + t_f - t') \\ & + \hat{K}(t')\, S(t_0 + t_f - t')\, \hat{K}(t') - Q(t_0 + t_f - t')\end{aligned} \tag{A.3}$$

has a unique symmetric positive definite solution $\hat{K}(t')$ satisfying the end con-

dition $\hat{K}(t_f) = \Gamma$. By substituting $t' = t_0 + t_f - t$, we have the symmetric negative definite solution $N(t) \equiv -\hat{K}(t_0 + t_f - t)$ that uniquely satisfies (17) with $N(t_0) = -\Gamma$. Moreover, the linear optimal control problem formulated as (A.1) and (A.2) shows that $\dot{\rho}(t) = [A(t) - S(t) N(t)] \rho(t)$ is uniformly asymptotically stable in reverse time.

Proof of Theorem 6. Let $y(t)^T = [z(t)^T \ \lambda(t)^T]$, $\zeta(t)^T = [\sigma(t)^T \ \rho(t)^T]$ and

$$W(t) = \begin{bmatrix} I & I \\ P(t) & N(t) \end{bmatrix}, \ L(t) = \begin{bmatrix} A(t) & -S(t) \\ -Q(t) & -A(t)^T \end{bmatrix},$$

$$D(t) = \begin{bmatrix} A(t) - S(t)P(t) & 0 \\ 0 & A(t) - S(t)N(t) \end{bmatrix}.$$

Suppose the transformation $y(t) = W(t)\zeta(t)$ maps $\dot{y}(t) = L(t) y(t)$ into $\dot{\zeta}(t) = D(t)\zeta(t)$, then

$$\dot{W}(t) = L(t) W(t) - W(t) D(t). \tag{A.4}$$

We consider the original system as the state-costate dynamics in (16) and construct $W(t)$ as in the dichotomy transformation (20), which leads to the block diagonal structure of $D(t)$. Substituting (16), (17), and (20) into (A.4), verifies that the transformed system is given by:

$$\begin{bmatrix} \dot{\sigma}(t) \\ \dot{\rho}(t) \end{bmatrix} = \begin{bmatrix} A(t) - S(t) P(t) & 0 \\ 0 & A(t) - S(t) N(t) \end{bmatrix} \begin{bmatrix} \sigma(t) \\ \rho(t) \end{bmatrix}. \tag{A.5}$$

Let the general solutions associated with (A.5) be expressed as:

$$\sigma(t) = \Theta(t)\,\sigma(t_0) \tag{A.6a}$$

$$\rho(t) = \Lambda(t)\,\rho(t_f) \tag{A.6b}$$

where $\Theta(t)$ and $\Lambda(t)$ are fundamental matrices. Then, for a particular set of boundary conditions of (16) we can write:

$$\begin{aligned} y(t_0) &= \sigma(t_0) + \Lambda(t_0)\,\rho(t_f) \\ y(t_f) &= \Theta(t_f)\,\sigma(t_0) + \rho(t_f) \end{aligned}$$

Consider two cases:

1. $I - \Theta(t_f)\,\Lambda(t_0)$ is singular with n_+ positive singular values, π_i, and $U\Pi V^T$ from the singular value decomposition of $I - \Theta(t_f)\,\Lambda(t_0)$. This leads to $y(t_0) = \sigma(t_0) + \Lambda(t_0)\,\rho(t_f)$ and $y(t_f) = \Theta(t_f)\,\sigma(t_0) + \sum_{i=1}^{n_+} \pi_i u_i v_i^T \rho(t_f)$.
2. $I - \Theta(t_f)\,\Lambda(t_0)$ is nonsingular, which yields:

$$\begin{bmatrix} \sigma(t_0) \\ \rho(t_f) \end{bmatrix} = \begin{bmatrix} I & \Lambda(t_0) \\ \Theta(t_f) & I \end{bmatrix}^{-1} \begin{bmatrix} y(t_0) \\ y(t_f) \end{bmatrix}. \tag{A.7}$$

For both cases, it can be concluded that the state-costate dynamics are transformed into two solutions $\sigma(t)$ and $\rho(t)$ that are uniformly asymptotically stable in forward time and reverse time, respectively. Moreover, when $I - \Theta(t_f)\,\Lambda(t_0)$ is nonsingular, (20), (A.6) and (A.7) yield the following solution in terms of the boundary conditions of the original Hamiltonian BVP (16):

$$\begin{bmatrix} z(t) \\ \lambda(t) \end{bmatrix} = \begin{bmatrix} I & I \\ P(t) & N(t) \end{bmatrix} \begin{bmatrix} \Theta(\mathrm{t}) & 0 \\ 0 & \Lambda(t) \end{bmatrix} \begin{bmatrix} I & \Lambda(t_0) \\ \Theta(t_f) & I \end{bmatrix}^{-1} \begin{bmatrix} z(t_0) \\ z(t_f) \end{bmatrix}. \tag{A.8}$$

Appendix B.

In this appendix, the relevant definitions of ISS and nonlinear programming properties for robust NMPC are given. Furthermore, the continuity property of the optimal solutions for the reformulated robust NMPC problem will be established, which in turn leads to the robustness of the infinite horizon NMPC approach.

Definition 10. *(Input-to-state stability) The system is ISS in $\mathcal{X}$ if there exist a $\mathcal{KL}$ function β and a $\mathcal{K}$ function γ such that for all $z_0 \in \mathcal{X}$ and $k \geq 0$,*

$$|x_k| \leq \beta\left(|x_0|, k\right) + \gamma\left(\|w\|\right). \tag{B.1}$$

Definition 11. *(ISS-Lyapunov function) A function $V(\cdot)$ is called an ISS-Lyapunov function if there exist some $\mathcal{K}_\infty$ functions α_1, α_2, α_3 and a $\mathcal{K}$ function σ such that for all $x \in \mathcal{X}$ and $w \in \mathcal{W}$,*

$$\begin{aligned} &\alpha_1\left(|x|\right) \leq V\left(x\right) \leq \alpha_2\left(|x|\right) \\ &V\left(\hat{F}\left(x,u,w\right)\right) - V\left(x\right) \leq -\alpha_3\left(|x|\right) + \sigma\left(|w|\right). \end{aligned} \tag{B.2}$$

Consider the NMPC problem (21) rewritten as:

$$\min_{y} \quad \phi\left(y;p\right) \tag{B.3a}$$

$$s.t. \quad c\left(y;p\right) = 0 \tag{B.3b}$$

$$g\left(y;p\right) \leq 0 \tag{B.3c}$$

where $y = (z_0, \ldots, z_N, v_0, \ldots, v_{N-1})$ and $p = x_k$. The following nonlinear programming properties are given to facilitate our analysis.

Definition 12. *(KKT) A point y^* is called a KKT-point for problem (B.3) if*

there exist multipliers λ and η which satisfy

$$\nabla\phi\left(y^*\right)+\nabla c\left(y^*\right)\lambda+\nabla g\left(y^*\right)\eta=0 \tag{B.4a}$$

$$c\left(y^*;p\right)=0 \tag{B.4b}$$

$$g\left(y^*;p\right)\leq 0 \tag{B.4c}$$

$$\eta^T g\left(y^*;p\right)=0 \tag{B.4d}$$

$$\eta\geq 0. \tag{B.4e}$$

We also define the Lagrange function of (B.3) as $\mathcal{L}=\phi\left(y;p\right)+\lambda^T c\left(y;p\right)+\eta^T g\left(y;p\right)$, the set of all multipliers λ and η which satisfy the KKT conditions (B.4) for a parameter p is $\mathcal{M}\left(p\right)$, and the active inequality constraint set is given by $J=\{j|g_j\left(y^*;p\right)=0\}$.

Definition 13. *(MFCQ) For problem (B.3), the Mangasarian-Fromovitz constraint qualification (MFCQ) holds at the optimal point y^* if and only if a) $\nabla c\left(y^*;p\right)$ is linearly independent, and b) there exists a vector q such that*

$$\begin{aligned}&\nabla c(y^*;p)^T q=0\\&\nabla g_j(y^*;p)^T q<0\ \forall j\in J.\end{aligned} \tag{B.5}$$

Definition 14. *(GSSOSC) The generalized strong second-order sufficient condition (GSSOSC) holds at the optimal point y^* if*

$$q^T\nabla_{yy}\mathcal{L}\left(y^*,\lambda,\eta;p\right)q>0\ \forall q\neq 0 \tag{B.6}$$

such that

$$\begin{aligned}&\nabla c_i(y^*;p)^T q=0,\ i=1,\ldots,n_c\\&\nabla g_j(y^*;p)^T q=0,\ \forall j\in\{j|j\in J,\eta_j>0\}\end{aligned} \tag{B.7}$$

holds for all multipliers $\lambda, \eta \in \mathcal{M}(p)$.

At the nonlinear programming solution, GSSOSC requires satisfaction of the strong second-order sufficient condition for each pair of multipliers (λ, η) in the bounded set defined under MFCQ. This can always be enforced by adding a regularization term $\|y - y^*\|^2_{\mathcal{Y}}$ to the objective of (B.3) with the matrix $\mathcal{Y}$ sufficiently positive definite.

The infinite horizon NMPC problem is reformulated as (36) to ensure that the nonlinear programming problem solved online satisfies MFCQ, and therefore the objective function V^r used to show stability is uniformly continuous in x. The proof for Theorem 9 is given as follows.

Consider the constraints of (36) rewritten as:

$$z_0 = x_k \tag{B.8a}$$

$$z_{l+1} = F(z_l, v_l), \ l = 0, \dots N-2 \tag{B.8b}$$

$$z_e = \bar{F}(z_N, \bar{v}) \tag{B.8c}$$

$$z_e + \hat{z} = z_s \tag{B.8d}$$

$$G_x(z_l) \leq 0, \ l = 0, \dots N \tag{B.8e}$$

$$G_u(v_l) \leq 0, \ l = 0, \dots N-1 \tag{B.8f}$$

$$G_u(\bar{v}) \leq 0, G_z(z_e, \hat{z}) \leq 0 \tag{B.8g}$$

Linearizing the equality constraints and the active inequality constraints of (B.8) at the optimum results in:

$$M_z d_z + M_v d_v = 0 \tag{B.9a}$$

$$N^J_{x,z} d_z \leq 0 \tag{B.9b}$$

$$N^J_{u,v} d_v \leq 0 \tag{B.9c}$$

where d_z and d_v are search directions of the states and controls, and the related matrices take the following form:

$$M_z = \begin{bmatrix} I & & & & & & \\ -F_z^0 & I & & & & & \\ & -F_z^1 & I & & & & \\ & & \ddots & \ddots & & & \\ & & & -\bar{F}_z^N & I & & \\ & & & & I & I \end{bmatrix} \tag{B.10a}$$

$$M_v = \begin{bmatrix} 0 & & & & & \\ -F_v^0 & & & & & \\ & -F_v^1 & & & & \\ & & \ddots & & & \\ & & & -\bar{F}_v^N & & \\ & & & & 0 \end{bmatrix} \tag{B.10b}$$

$$N_{x,z}^J = diag\left\{G_{x,z}^{j_0}, G_{x,z}^{j_1}, \ldots, G_{x,z}^{j_N}, G_{x,z}^{j_e}\right\} \tag{B.10c}$$

$$N_{u,v}^J = diag\left\{G_{u,v}^{j_0}, G_{u,v}^{j_1}, \ldots, G_{u,v}^{j_N}, G_{u,\bar{v}}^{j}\right\} \tag{B.10d}$$

where F_z^l, $\bar{F}_z^l$, F_v^l, and $\bar{F}_v^l$ denote the Jacobians of $F\left(z_l, v_l\right)$ and $\bar{F}\left(z_l, v_l\right)$ with respect to the variables z_l and v_l, $G_{x,z}^{J_l}$ is the Jacobian of the active constraints of G_x at time step l, and $G_{u,v}^{J_l}$ is the Jacobian of the active constraints of G_u at time step l. The submatrices $G_{x,z}^{j_l}$ and $G_{u,v}^{j_l}$ may be of variable dimension or be empty, depending on whether the associated inequality constraints are active or inactive. It can be concluded that the submatrices F_z^l and $\bar{F}_z^l$ are square and nonsingular, and the matrix $\nabla c^T = \begin{bmatrix} M_z & M_v & 0 \end{bmatrix}$ is full row rank, which implies that the equality constraint gradients are linearly independent. Moreover, the relaxation of the active state inequalities of (36) at the optimum

results in:

$$N_{x,z}^J d_z - E_{J,x} d_\varepsilon \leq 0 \tag{B.11a}$$

$$-d_\varepsilon \leq 0 \tag{B.11b}$$

$$N_{u,v}^J d_v \leq 0 \tag{B.11c}$$

where ε denotes the concatenation of the slack variables, and the gradients of the active inequality constraints are given by:

$$\nabla g_J^T = \begin{bmatrix} N_{x,z}^J & 0 & -E_J \\ 0 & 0 & -I \\ 0 & N_{u,v}^J & 0 \end{bmatrix} \tag{B.12}$$

where E_J consists of the rows of the identity matrix corresponding to the active state inequalities. Since the control set $\mathcal{U}$ is convex and has an interior, there exists some d_v^0 such that $G_u^j\left(v^* + d_v^0\right) < 0 \ \forall j \in J$. As a result of Taylor's theorem, we have

$$G_u^j\left(v^* + d_v^0\right) = G_u^j\left(v^*\right) + \nabla G_u^j (v^*)^T d_v^0 + \frac{1}{2}\left(d_v^0\right)^T \nabla^2 G_u^j\left(v^* + s d_v^0\right) d_v^0 < 0 \tag{B.13}$$

for $j \in J$ and some $s \in [0,1]$. Since $G_u^j\left(v^*\right) = 0$ and by convexity we have

$$\frac{1}{2}\left(d_v^0\right)^T \nabla^2 G_u^j\left(v^* + s d_v^0\right) d_v^0 \geq 0 \tag{B.14}$$

then it follows from (B.13) that:

$$\nabla G_u^j (v^*)^T d_v^0 = G_u^j\left(v^* + d_v^0\right) - \frac{1}{2}\left(d_v^0\right)^T \nabla^2 G_u^j\left(v^* + s d_v^0\right) d_v^0 < 0 \tag{B.15}$$

which implies $N_{u,v}^J d_v^0 < 0$. Next, we consider the vector $q^T = \begin{bmatrix} d_z^T & d_v^T & d_\varepsilon^T \end{bmatrix}$

with $d_z = -M_z^{-1} M_v d_v^0$ from (B.9a) and $d_v = d_v^0$. For a given d_v^0, d_ε can be selected in the following manner:

$$E_J d_\varepsilon > N_{x,z}^J d_z. \tag{B.16}$$

The derivation shows that $\nabla \mathrm{c}^T q = 0$ and $\nabla g_J^T q < 0$ as required in Definition13. Consequently, MFCQ is satisfied for the reformulated problem (36).

References

[1] J. Berberich, J. Köhler, M. A. Müller, F. Allgöwer, Data-driven model predictive control: closed-loop guarantees and experimental results, at - Automatisierungstechnik 69 (7) (2021) 608–618. doi:doi:10.1515/auto-2021-0024.

[2] F. Borrelli, A. Bemporad, M. Morari, Predictive control for linear and hybrid systems, Cambridge University Press, 2017.

[3] V. M. Zavala, L. T. Biegler, The advanced-step nmpc controller: Optimality, stability and robustness, Automatica 45 (1) (2009) 86–93. doi:https://doi.org/10.1016/j.automatica.2008.06.011.
URL https://www.sciencedirect.com/science/article/pii/S0005109808004196

[4] S. Keerthi, E. Gilbert, Optimal infinite-horizon feedback laws for a general class of constrained discrete-time systems: stability and moving-horizon approximations, J. of Optimization Theory and Applications 57 (1988) 265–293.

[5] D. Limon, T. Alamo, F. Salas, E. F. Camacho, On the stability of constrained mpc without terminal constraint, IEEE transactions on automatic control 51(5) (2006) 832–836.

[6] M. Alamir, Contraction-based nonlinear model predictive control formulation without stability-related terminal constraints, Automatica 75 (2017) 288–292.

[7] M. Alamir, Stability proof for nonlinear mpc design using monotonically increasing weighting profiles without terminal constraints, Automatica 87 (2018) 455–459.

[8] M. Alamir, G. Pannocchia, A new formulation of economic model predictive control without terminal constraint, Automatica 125 (2021) 109420.

[9] G. Pannoccia, Robust model predictive control with guaranteed setpoint tracking, Journal of Process Control 14 (2004) 927–937.

[10] G. Pannocchia, S. Wright, J. Rawlings, Existence and computation of infinite horizon model predictive control with active steady-state input constraints, IEEE Transactions on Automatic Control 48(6) (2003).

[11] T. Faulwasser, G. Pannocchia, Toward a unifying framework blending real-time optimization and economic model predictive control, Ind. Eng. Chem. Res. 58 (2019) 13598.

[12] J. Leung, F. Permenter, I. V. Kolmanovsky, A stability governor for constrained linear-quadratic mpc without terminal constraints, Automatica 164 (2024) 111650.

[13] M. Polver, D. Limon, F. Previdi, A. Ferramosca, Robust contraction-based model predictive control for nonlinear systems, arXiv:2502.02394 (2025).

[14] H. Chen, F. Allgöwer, A quasi-infinite horizon nonlinear model predictive control scheme with guaranteed stability, Automatica 34 (1998) 1205–1217.

[15] C. V. Rao, J. B. Rawlings, D. Q. Mayne, Constrained state estimation for nonlinear discrete-time systems: Stability and moving horizon approximations, IEEE Trans. Auto. Cont. 48(2) (2003) 246–258.

[16] C. Rajhans, S. Gupta, Practical implementable controller design with guaranteed asymptotic stability for nonlinear systems, Computers & Chemical Engineering 163 (2022) 107827.

[17] S. Gupta, C. Rajhans, Application of terminal region enlargement approach for discrete time quasi infinite horizon nonlinear model predictive control, International Journal of Adaptive Control and Signal Processing 38, 5 (2024) 1543 – 156.

[18] D. Limon, Control predictivo de sistemas no lineales con restricciones: estabilidad y robustez, Universidad de Sevilla, 2002.

[19] A. Krener, Adaptive horizon model predictive control and albrekht's method, Encyclopedia of Systems and Control (2021) 27–40.

[20] D. W. Griffith, S. C. Patwardhan, L. T. Biegler, Robustly stable adaptive horizon nonlinear model predictive control, Journal of Process Control 70 (2018) 109–122.

[21] P. Kunkel, O. von dem Hagen, Numerical solution of infinite-horizon optimal-control problems, Computational Economics 16(3) (2000) 189–205.

[22] J. Marutani, T. Ohtsuka, A real-time algorithm for nonlinear infinite horizon optimal control by time axis transformation method, Int. J. Robust Nonlinear Control 23 (2013) 1955–1971.

[23] L. Würth, W. Marquardt, Infinite-horizon continuous-time nmpc via time transformation, IEEE Trans. Aut. Cont. 59 (2014) 2543–2548.

[24] W. M. L. Würth, I. J. Wolf, On the numerical solution of discounted economic nmpc on infinite horizons, IFAC Proceedings Volumes 46(32) (2013) 209–214.

[25] L. Würth, I. J. Wolf, W. Marquardt, On the numerical solution of discounted economic nmpc on infinite horizons, IFAC Symposium on Dynamics and Control of Process Systems (2013) 209–214.

[26] M. Muehlenbach, R. Andrea, Parametrized infinite-horizon model predictive control for linear time-invariant systems with input and state constraints, Proceedings ACC (2016) 2669 – 2674.

[27] M. Muehlebach, C. Sferrazza, R. Andrea, Implementation of a parametrized infinite-horizon model predictive control scheme with stability guarantees, IEEE International Conference on Robotics and Automation (ICRA) (2017).

[28] W. B. Greer, C. Sultan, Infinite horizon model predictive control tracking application to helicopters, Aerospace Science and Technology 98 (2020) 10567.

[29] R. R. Wilde, P. Kokotovic, A dichotomy in linear control theory, IEEE Trans. Aut. Control 17 (1972) 382–383.

[30] U. Ascher, R. M. Mattheij, R. D. Russell, Numerical Solution of Boundary Value Problems for Ordinary Differential Equations, Prentice-Hall, 1988.

[31] T. van Keulen, Solution for the continuous-time infinite-horizon linear quadratic regulator subject to scalar state constraints, IEEE Control Systems Letters 4(1) (2020) 133–138.

[32] R. E. Kalman, Contributions to the theory of optimal control, Boletin de la Sociedad Matematica Mexicana 5 (1960) 102–119.

[33] L. Grüne, Economic receding horizon control without terminal constraints, Automatica 49 (2013) 725–734.

[34] X. Yang, D. W. Griffith, L. T. Biegler, Nonlinear programming properties for stable and robust nmpc, IFAC-PapersOnLine 48(23) (2015) 388–397.

[35] I. Wolf, L. Würth, W. Marquardt, Rigorous solution vs. fast update: Acceptable computational delay in nmpc, Decision and Control and European Control Conference Orlando, Florida, USA (2011) 5230–5235.

[36] M. L. Bynum, G. A. Hackebeil, W. E. Hart, C. D. Laird, B. L. Nicholson, J. D. Siirola, J.-P. Watson, D. L. Woodruff, Pyomo: Optimization Modeling in Python, 3rd Edition, Vol. 67, Springer Science & Business Media, 2021.

[37] H. S. Fogler, Elements of Chemical Reaction Engineering, Prentice-Hall, Upper Saddle River, NJ, 2025.

[38] C. Green, Equations of motion for the cart and pole control task, `https://sharpneat.sourceforge.io/research/cart-pole/cart-pole-equations.html`, accessed: 2025-04-29.

[39] R. Lopez-Negrete, F. J. D'Amato, L. T. Biegler, A. Kumar, Fast nonlinear model predictive control: Formulation and industrial process applications, Computers and Chemical Engineering 51 (2013) 55–64.